

QUANTITATIVE ASSESSMENT OF CHANGES IN CELLULAR MORPHOLOGY
AND CELL DIVISION NUMBER DURING TELOMERE-INITIATED
SENESCENCE IN THE YEAST *SACCHAROMYCES CEREVISIAE*

by

Shubha Rajya Laxmi Malla, B.S.

A thesis submitted to the Graduate Council of
Texas State University in partial fulfillment
of the requirements for the degree of
Master of Science
with a Major in Biochemistry
December 2016

Committee Members:

L. Kevin Lewis, Chair

Wendi M. David

Liqin Du

COPYRIGHT

by

Shubha Rajya Laxmi Malla

2016

FAIR USE AND AUTHOR'S PERMISSION STATEMENT

Fair Use

This work is protected by the Copyright Laws of the United States (Public Law 94-553, section 107). Consistent with fair use as defined in the Copyright Laws, brief quotations from this material are allowed with proper acknowledgment. Use of this material for financial gain without the author's express written permission is not allowed.

Duplication Permission

As the copyright holder of this work I, Shubha Rajya Laxmi Malla, authorize duplication of this work, in whole or in part, for educational or scholarly purposes only.

ACKNOWLEDGEMENTS

I would like to express my sincere gratitude towards my academic advisor Dr. L. Kevin Lewis for constant guidance and support, and the opportunity to work in his laboratory. Dr. Lewis' valuable teachings and trainings have helped me tremendously to sharpen and broaden my knowledge in the field of Biochemistry. I would also like to thank Dr. Wendi M. David and Dr. Liqin Du for their support and guidance throughout my project and my academic career. Members of Dr. Lewis' research lab have always been there to support me and maintain a healthy environment to grow academically. My dad, mom and brother's immense love and support has always encouraged me to do better and stay focused. My friends and loved ones always stayed by my side. I also would like to thank the entire Chemistry and Biochemistry Department and Texas State University family for their support and encouragement during my graduate studies.

TABLE OF CONTENTS

	Page
ACKNOWLEDGEMENTS	iv
LIST OF TABLES	vi
LIST OF FIGURES	vii
CHAPTER	
I. INTRODUCTION	1
II. MATERIALS AND METHODS	9
III. RESULTS AND DISCUSSION.....	20
IV. SUMMARY AND CONCLUSIONS.....	61
REFERENCES	65

LIST OF TABLES

Table	Page
1. List of <i>Saccharomyces cerevisiae</i> strains used for this project	12
2. List of PCR primer sequences used for this project	12
3. List of plasmids used for this project	12
4. The number of full columns on the 4 th streak of <i>est2</i> cells (YLKL803) grown on rich media in previous experiments	28
5. The number of full columns on the 4 th streak of <i>est2</i> cells (YLKL803) grown on rich media performed for the current project	29
6. The number of full columns of growth on the 4 th streak of <i>est2</i> cells (YLKL961) containing pVL715	32
7. The total number of cells in a single colony for each generation of growth	33
8. The number of generations that cells went through during each streak of <i>est2</i> cells on rich media using a Pasteur pipette.....	36
9. The number of generations that cells went through during each streak of <i>est2</i> cells on rich media using a 1 ml plastic pipette.....	36
10. The number of generations that cells went through during each streak of <i>est2</i> cells on synthetic media using a Pasteur pipette	37
11. The number of generations that cells went through during each streak of <i>est2</i> cells on synthetic media using a 1 ml plastic pipette	37
12. The number of generations that cells went through during each streak of <i>est2 rad 52</i> cells on rich media using a 1 ml plastic pipette	38
13. The number of generations that cells went through during each streak of <i>est2 rad 52</i> cells on synthetic media using a 1 ml plastic pipette	38
14. Percent change in sizes of <i>est2 rad52</i> cells on rich YPDA media measured using 1000X magnification.....	51

LIST OF FIGURES

Figure	Page
1. Diagram showing replication of telomeric DNA by telomerase complex (7).....	2
2. Telomerase complexes of the yeast <i>Saccharomyces cerevisiae</i> and humans (6).....	4
3. Diagram showing homologous recombination (genetic exchange) increasing the length of a short telomere (19).....	6
4. Diagram showing the yeast strain YLKL803 with a plasmid containing <i>EST2</i> polymerase under the control of a galactose regulated promoter	21
5. Diagram showing the historical method of streaking double columns of cells for solid media-based senescence assays	22
6. Diagram illustrating the stochastic process of senescence	23
7. The new statistics-based senescence assay developed in this lab by Naoko Araki and Neda Ghanem (19, 29)	24
8. The new statistics-based senescence assay uses a printed grid system (placed under the plate to be streaked) for streaking cells as long single columns	25
9. Diagram showing the typical size of a colony picked for each senescence cell streak	26
10. Examples of plate streaks performed for the new senescence assay	27
11. Schematic diagram illustrating an alternative method for conducting senescence assays	31
12. Diagram showing multiple divisions of a single cell to form a colony.....	33
13. New method using 1 ml plastic pipette with an attached electronic pipet aid to core colonies	35
14. Cells increase in size during senescence, but the magnitudes of these changes have never been measured (16, 18, 20)	39
15. Comparison of normal and senescent cells	40

16. Measurement of the sizes of normal and senescent (4 th streak) unbudded cells on rich media (YPDA) using the phase contrast microscope with a 40X objective (400X magnification)	41
17. Measurement of the sizes of unbudded cells after each streak on rich media (YPDA) using the phase contrast microscope with 400X magnification.....	42
18. Measurement of the sizes of wildtype and senescent (4 th streak) budded cells on rich media (YPDA) using 400X magnification.....	43
19. Measurement of the sizes of budded cells after each streak on rich media (YPDA) at 400X magnification.....	43
20. Yeast cells appear larger using a 100X objective than with a 40X objective	44
21. Measurement of the sizes of wildtype and senescent (4 th streak) unbudded cells on rich media (YPDA) using 1000X magnification	45
22. Measurement of the sizes of unbudded cells after each streak on rich media (YPDA) using 1000X magnification	45
23. Measurement of the sizes of wildtype and senescent (4 th streak) budded cells on rich media (YPDA) using 1000X magnification.....	46
24. Measurement of the sizes of budded cells after each streak on rich media (YPDA) using 1000X magnifications	46
25. Measurement of the sizes of normal and senescent (4 th streak) unbudded cells on synthetic media (glucose complete) using 1000X magnification	47
26. Measurement of the sizes of unbudded cells after each streak on synthetic media (glucose complete) using 1000X magnification	47
27. Measurement of the sizes of normal and senescent (4 th streak) budded cells on synthetic media (glucose complete) at 1000X magnification	48
28. Measurement of the sizes of budded cells after each streak on synthetic media (glucose complete) using 1000X magnification	48
29. In <i>est2 rad52</i> cells, senescence occurs on the 3 rd streak rather than on the 4 th streak (16)	49

30. Measurement of the sizes of normal and senescent (4 th streak) cells on rich media (YPDA) using 1000X magnification	50
31. Measurement of the sizes of normal and senescent (4 th streak) cells of all kinds on rich media (YPDA) using 1000X magnification	51
32. Schematic illustration of sedimentation of normal and senescent cells	52
33. Senescent (<i>est2</i>) cells exhibit higher OD ₆₀₀ values than wildtype cells.....	53
34. Older cells sediment more rapidly than normal cells	54
35. Older cells sediment more rapidly than normal cells after growth in synthetic media too.....	56
36. Measurement of changes in the OD ₆₀₀ of <i>est2 rad52</i> cells at cell titer of 1×10^7 cells/ml after growth on rich media (YPDA).....	57
37. Creation of a hypersensitive strain	59
38. Gel picture showing proper insertion of the <i>Nat^r</i> gene into the <i>PDR5</i> locus in two isolates.....	60

I. INTRODUCTION

The ends of eukaryotic chromosomes are protected by specialized protein caps at chromosome regions called telomeres that help to maintain the stability of the DNA. Telomeres protect chromosomes from degradation by nuclease enzymes and prevent chromosomes from fusing end to end (1). Telomere DNA consists of many repeats of short sequences. For example, human telomeres consist of thousands of copies of the short DNA sequence TTAGGG (2). Telomeric DNA repeat sequences are replicated by telomerase, which was first characterized by Greider and Blackburn (3). Greider *et al.* (1985) found a novel transferase-like activity in *Tetrahymena* cell free extracts that added telomeric repeat sequences onto synthetic primers (3, 4). This enzyme, called telomerase, is an end-specific RNA-dependent DNA polymerase complex that helps to maintain the lengths of telomeres. It has reverse transcriptase activity that adds telomeric repeat sequences to the 3' end of each chromosome strand during S phase of the cell cycle (4). The telomerase complex replicates telomeric DNA by binding to the ends and annealing its RNA to the DNA and using the RNA strand as a template to synthesize new DNA (Figure 1). This enzyme is critical to overcome the “end replication problem”. During each cell division, the major DNA polymerases in the cell cannot replicate the very ends of the chromosomes, resulting in shortening of the telomeres if telomerase is not present. In every cell cycle the telomere lengths get shorter and shorter due to the end replication problem (5, 6).

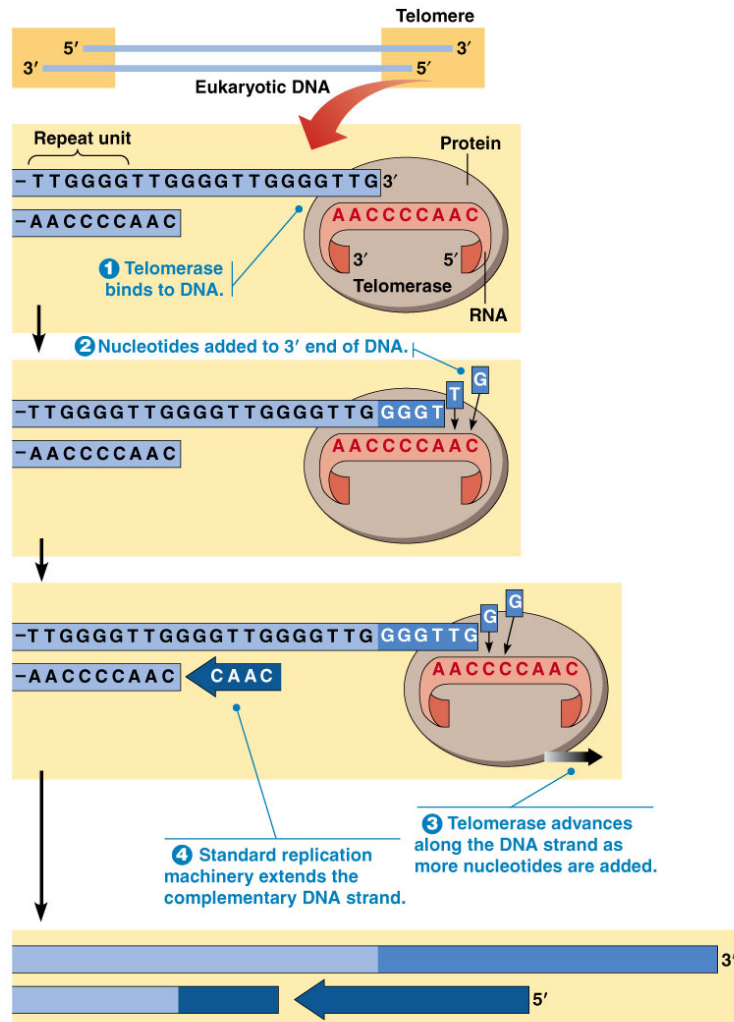


Figure 1. Diagram showing replication of telomeric DNA by telomerase complex (7).

Most human cells stop making telomerase during embryonic development, which causes progressive telomere shortening as humans age. Younger individuals are known to have longer telomeres than older people. At the time of birth, the average length of telomeres is about 8,000 – 10,000 base-pairs (bp). However, by the time individuals are 70 years old, telomere lengths get reduced to an average size of about 3,000 bp (5). Humans of the same age can have different telomeric lengths. Past studies have shown

that older people with the shortest telomeres are at higher risk of developing age-related diseases (5). Studies have also associated shorter telomeres with reduced cognitive function in older humans (8). Several studies have shown that telomere lengths are affected by lifestyle choices. For example, rates of telomere shortening are increased in active smokers relative to non-smoking individuals (9) and telomere length is preserved in healthy older adults who perform regular vigorous aerobic exercise (10). Proper diet and nutrition also has a positive impact on telomere length (11). Although most human cells do not produce telomerase, approximately 90% of cancer cells reactivate telomerase expression, which results in immortalization of the cells (12). Recent work has targeted telomeres and telomerase for cancer therapy (13).

Saccharomyces cerevisiae, also known as budding yeast, is a good experimental model to study the aging process because it has a small number of genes (~6000), many proteins are similar to human proteins, and it has the ability to grow in either a haploid or diploid state. The cell cycle of budding yeast is short compared to cultured human cells, and yeast cells double approximately every 90 minutes at 30°C. One can do complex genetic studies in yeast as well. Moreover, the telomerase complex of yeast is analogous to the telomerase complex of humans (Figure 2) (14). Eukaryotic telomerase complexes consist of protein subunits plus an RNA component. Yeast telomerase consists of Est1, Est2, and Est3 as protein subunits and *TLC1* as the RNA subunit. Est2 is the catalytic subunit of yeast telomerase. In humans, the catalytic subunit is called hTERT (15).

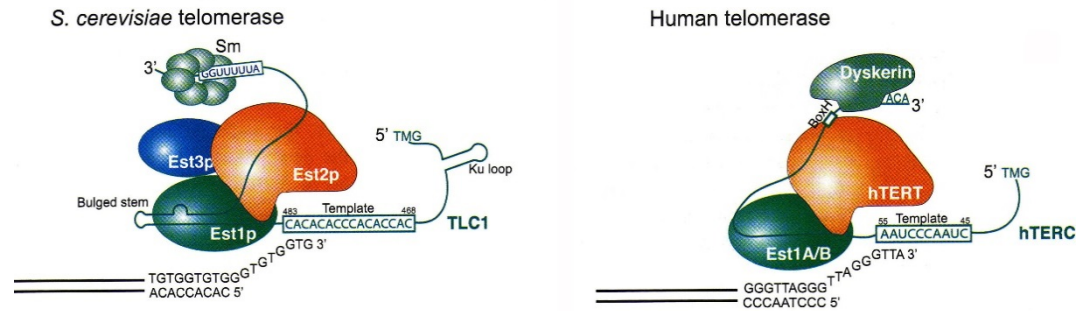


Figure 2. Telomerase complexes of the yeast *Saccharomyces cerevisiae* and humans (6).

Human somatic cells grown in culture undergo approximately 50 cell divisions before they stop growing; this is called telomere-initiated cellular senescence or *in vitro* cell aging. Cellular senescence is due to progressive telomere shortening in the cells caused by an absence of telomerase (15). In contrast to human cells, yeast cells normally produce telomerase and do not exhibit cellular senescence. Inactivation of the *EST2* gene, which encodes the telomerase polymerase subunit, causes yeast cells to exhibit progressive telomere shortening and senescence (loss of growth capacity), similar to human cells. In budding yeast, the cells undergo senescence after approximately 60 – 70 generations (cell cycles) (16, 17, 18). Senescence is a random process and some cells senesce faster or slower than others.

In Dr. Lewis' laboratory, new yeast strains and improved statistics-based senescence assays have been developed that allow one to quantitate rates of cell aging (16, 19). Recent work has demonstrated the usefulness of the new method for studying the roles of several DNA repair genes in cell aging (19). A yeast strain was developed for the experiments that allow controlled expression of the *EST2* gene (16). A plasmid containing *EST2* under the control of a galactose-regulated promoter is present in the

cells. When grown in galactose media, the cells produce telomerase and are immortal. After transfer to glucose media, telomerase synthesis is halted and the cells undergo senescence.

Past studies have shown that there is an association between telomere shortening and oxidative damage. Reactive oxygen species (ROS) produced during normal cellular metabolism can cause oxidative stress and DNA damage in cells, potentially increasing the rate of telomere shortening (20-23). The effect of ROS are normally decreased through the actions of antioxidant enzymes such as superoxide dismutases, catalases and glutathione peroxidases, and therefore cells containing mutations in the genes encoding these enzymes experience higher levels of damage to DNA and other biomolecules.

Chromosomal DNA gets damaged frequently due to its sensitivity to ultraviolet light, ionizing radiation and other internal chemicals. DNA damaging agents cause lesions in DNA and are dangerous and may lead to mutation and age-related diseases. A major type of DNA lesion is known as a double-strand break (DSB). It is very critical to repair DNA DSBs for the maintenance of the genome (24). Every eukaryotic cell has repair pathways for DSBs and several genes and proteins are involved in these complex pathways. Non-homologous DNA end-joining (NHEJ) and homologous recombination (HR) are the two major DSB repair mechanisms.

NHEJ involves the direct rejoining of broken DNA ends without using a repair template. However, homologous recombination uses a sister chromatid or a homologous chromosome as repair template (25). In yeast, several genes collectively known as the RAD52 group are involved in homologous recombination (26). Characterization of yeast genes involved in recombination pathways are critical due to their homology to human

genes that have been implicated in several human genetic disorders and cancer (27). The process of exchange of genetic information between similar sequences is called homologous recombination and it is also crucial for maintaining telomere lengths (25). Past studies have shown that inactivation of the *RAD52* gene accelerates cellular senescence when compared to wild type cells, indicating that *RAD52* plays an important role in reducing the rate of telomere shortening through the homologous recombination pathway (16, 19, 28). For example, homologous recombination occurs as shown in Figure 3, whereby telomeres may undergo unequal genetic exchange with each other so that smaller telomeres are lengthened by exchange with longer telomeres (19).

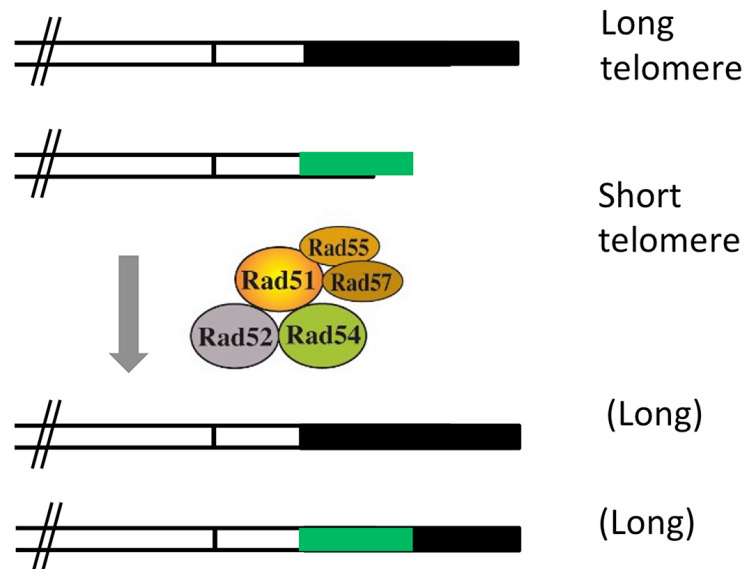


Figure 3. Diagram showing homologous recombination (genetic exchange) increasing the length of a short telomere (19).

The major goal of this project was to perform a quantitative assessment of changes in cellular morphology and cell division number during telomere-initiated senescence. First, I completed the development and testing of new quantitative assays to monitor senescence initiated by Naoko Araki and Neda Ghanem (19, 29). Initial work that I have done has focused on (a) accurately calculating, for the first time, the actual average number of generations (cell divisions) cells undergo during senescence using both rich media and synthetic (defined) cell growth media, (b) quantitating how the morphology of cells changes during senescence, especially cell size, using a video camera-linked phase contrast microscope, and (c) analyzing how the rates of sedimentation of cells change during senescence using light scattering and spectrophotometry. Using a video camera-linked phase contrast microscope one can obtain a detailed view of live, unstained transparent cells (30). These experiments have found that wild type cells undergo at least 63 generations before undergoing senescence, while telomerase and recombination-deficient *rad52* mutants undergo a minimum of only ~ 42 generations before senescence. Also, senescent cells progressively increased in size from approximately 6 μm in diameter to 10 μm during senescence. The changes in cell morphology caused the older cells to sediment out of solutions much more rapidly than normal cells. A consequence of this is that one needs to be very careful while working with senescent cells because their concentration is changing constantly due to cells sedimenting to the bottom of the tube.

An additional major goal of the project was to use the special senescence strain system to analyze the effects of altering chemical processes on senescence rates. In particular, chemical factors such as pro-oxidants and antioxidants that may accelerate or

slow the rate of senescence can be investigated. To do this most efficiently, the original *GALI-V10p::EST2* senescence strain was engineered to make it more sensitive to the presence of chemicals added to the cell growth medium. This was accomplished by knocking out the genes *SNQ2* and *PDR5*, which encode membrane-bound multidrug transporter proteins (33, 34). Cells lacking these transporters do not pump drugs out efficiently and therefore they accumulate higher levels of drugs inside the cells, allowing lower concentrations of the drugs to be added to the cells. Our hypothesis is that the new assay system will allow assessment of the impacts of genetic and chemical factors more quantitatively than has ever been done before.

II. MATERIALS AND METHODS

Materials

General reagents

Ethidium bromide (EtBr) was purchased from IBI Scientific (Peosta, IA). Agarose LE was obtained from Gold Biotechnology (St. Louis, MO). TAE (50X) buffer was obtained from Omega Bio-tek, Inc. (Norcross, GA). Ethylenediamine tetraacetic acid (EDTA) and glycerol were obtained from EMD Chemicals, Inc. (Darmstadt, Germany). Dimethyl sulfoxide (DMSO) and lithium acetate (LiAc) were purchased from Alfa Aesar (Ward Hill, MA). Isopropanol was obtained from VWR International (West Chester, PA). Polyethylene glycol (PEG 4000), and ampicillin were purchased from Sigma-Aldrich Chemical Co. (St. Louis, MO). Sodium dodecyl sulfate (SDS) and Tris base were obtained from J.T. Baker (Center Valley, PA). RNase A was obtained from Thermo Fisher Scientific (Santa Clara, CA). Sonicated salmon sperm carrier DNA was obtained from Agilent Technologies (Santa Clara, CA). 2-log DNA ladder and loading dye were purchased from New England Biolabs (Ipswich, MA). Ethanol was obtained from Texas State University (San Marcos, TX). QIAprep Spin Miniprep Kits were purchased from Qiagen (Hilden, Germany). Nourseothricin sulfate (Nat) was obtained from Gold Biotechnology, Inc. (St. Louis, MO) and was included in plates at a concentration of 108 µg/ml.

Yeast growth media

D-(+)-glucose and soy peptone were purchased from Amresco (Solon, OH). D-(+)- galactose was obtained from Acros Organics (Fair Lawn, NJ). All amino acids were purchased from Sigma-Aldrich Chemical Co. (St. Louis, MO). Bacto yeast extract was made by Becton Dickinson and Company (Sparks, MD). Molecular biology grade agar was purchased from Teknova (Hollister, CA).

Enzymes and PCR reagents

Taq DNA polymerase, dNTPs, 10X ThermoPol buffer and $MgCl_2$ were purchased from New England Biolabs (Ipswich, MA).

Cell Culture solutions media

Yeast cells were grown on YPDA (rich) plates (1% yeast extract, 2% soy peptone, 2% dextrose, 2.2% molecular biology grade agar and 0.001% adenine). YPDA broth was prepared the same way as YPDA plates, but without the agar. For synthetic media, 1 L of plates contained 0.5% ammonium sulfate, 0.17% yeast nitrogen base without amino acids or ammonium sulfate, 2% dextrose, 2.2% molecular biology grade agar, and 0.051% “10 amino acid mix”. The 10 amino acid mix contains arginine, aspartic acid, glutamic acid, isoleucine, methionine, phenylalanine, serine, threonine, tyrosine and valine. Before autoclaving, 12 ml 0.5% uracil, 10 ml 0.5% tryptophan, 10 ml 0.5% leucine, 5 ml 1% lysine, 2 ml 0.5% adenine and 2 ml 1% histidine were added to the solution. For synthetic media lacking amino acids or bases, one of these six amino acids or bases was not added to the solution to prepare plates. For example for preparation of glucose minus uracil

(Glu – ura) plates, all the amino acids and bases were added except uracil. LB plates were prepared by adding LB mix powder to ddH₂O, autoclaving, and pouring the plate with or without the addition of 100 µg/ml ampicillin. Likewise, TB broth was prepared by adding TB mix powder to ddH₂O and autoclaving.

Equipment

The incubator was purchased from VWR Scientific Products (Radnor, PA). Horizon 11-14 gel rigs were purchased from LabRepCo (Horsham, PA). The RED imaging system was obtained from ProteinSimple (San Jose, CA). The T100 Thermal Cycler was obtained from Bio-Rad Laboratories (Hercules, CA). The Sorvall Lynx 6000 centrifuge and Savant DNA 120 SpeedVac Concentrator were purchased from Thermo Fisher Scientific (Santa Clara, CA). The Sonics Vibra-cell Model VCX130 sonicator was purchased from Sonics and Materials, Inc. (Newton, CT).

Yeast strains and plasmids

All yeast strains used for this project were derived from BY4742 (*MAT α his3 Δ 1 leu2 Δ 0 lys2 Δ 0 ura3 Δ 0*) (Table 1). The sequences of all oligonucleotide primers are listed in Table 2. Plasmids used in this project were isolated from *E. coli* cells by alkaline lysis and are listed in Table 3.

Table 1. List of *Saccharomyces cerevisiae* strains used for this project.

Strain	Genotype	Reference
BY4742	<i>MATa ura3-Δ0 leu2-Δ0 lys2-Δ0 his3-Δ1</i>	35
YLKL803	BY4742, <i>est2Δ::HygB^r</i> + pLKL82Y [<i>URA3, CEN/ARS, GAL1-V10p::EST2</i>]	16
YLKL807	YLKL803, <i>rad52Δ::G418^r</i>	16
YLKL961	BY4742, <i>est2Δ::HygB^r</i> + pVL715 [2- micron <i>URA3 ADHIp::EST2</i>]	Lab strain
YLKL1556	YLKL803, <i>snq2Δ::G418^r</i>	Lab strain
YLKL1557	YLKL803, <i>pdr5Δ::G418^r</i>	Lab strain
YLKL1558	YLKL803, <i>snq2Δ::G418^r pdr5Δ::Nat^r</i>	This work
YLKL1580	BY4742, <i>pdr5Δ::Nat^r</i>	This work

Table 2. List of PCR primer sequences used for this project.

Primer	Sequence
gPDR5A	GTTGCGCTTGGAAGAACTTAAGTGCTTCTGGTGCTTCCGCAGAGTCG CCTATCATGTGACTGTCGCCCGTACATT
gPDR5B	ACCCCTTTCATGCAACTGGCCAGCTGCAGACGCGTTGGAGTAAAAT CCAATTGGACAAGTTCTTGAAAACAAGAATC
5-pdr5	CCGCTCGTTCGAAAGACTTTAGACAA
3-pdr5	GTTCCATGTACTGCCACATGTCATACC

Table 3. List of plasmids used for this project.

Plasmid	Genotype	Source
pAG25	<i>NAT1</i>	36
pLKL82Y	<i>URA3, CEN/ARS, GAL1-V10p::EST2</i>	16

Methods

Solid media-based senescence assays

Aging studies in telomerase-deficient YLKL803 cells (BY4742, *est2Δ::HygB^r* + pLKL82Y (*GAL1-V10p::EST2*) and *rad52* mutant strain YLKL807 (YLKL803, *rad52Δ::G418^r*) on synthetic and rich media was studied by performing assays with a series of streaks. Each streak for single colonies allowed measurement of the number of generations of growth the cell goes through. For the first streak, cells were picked from a freshly grown galactose minus uracil stock plate so that cells were producing telomerase from the *GAL1-V10p::EST2* plasmid initially. Cells were streaked on to either synthetic media or rich media as double columns using a template under the plate. For each plate 4 separate double columns were streaked. All second columns were streaked toward the outer edge of the plate to allow cells to have proper access to nutrients. Cells were then allowed to grow in a 30°C incubator for 2-4 days depending on growth media (synthetic media: 3-4 days, rich media: 2-3 days). For the second streak, an appropriately sized (~ 0.8 mm) single colony from the first streak was picked and streaked on to a fresh new plate and the process was repeated again. For the third streak, an appropriately sized (~ 0.8 mm) single colony from the second streak was picked to create double columns on the fresh new plate. Altogether, four separate double columns were streaked per plate and cells were allowed to grow in the incubator at 30°C for 3-4 days. Finally, for the fourth streak, 48 different individual colonies was picked and streaked as tall columns onto 6 different plates, creating 8 separate columns on each plate. The plates were incubated at 30°C for four days. As cells aged, the growth rate of the cells slowed down, which is why plates were incubated for 4 days on the 4th streak.

Counting the number of cells in each colony on senescence assay plates

A 1 ml plastic pipette with an attached electronic pipette aid was used to core all cells from a single colony of the right size (~ 0.8 mm). The pipette aid was used to pull the colony with agar from the Petri dish. After expulsion of the plug of agar, the plastic pipette was rinsed 3-4 times with ddH₂O from the recipient 1.5 ml microfuge tube, which contained 500 µl or 1000 µl of ddH₂O. The cells were vortexed hard for ~ 10 seconds to separate the cells from the agar and were then sonicated for ~ 10 seconds. The sonicator used sound waves to separate the cells from each other. A total of 12 µl – 16 µl of cells were transferred on to a hemocytometer, which was placed in a United Scope Model M837T video camera-linked phase contrast microscope (Hopewell Junction, NY) and cells were counted. Approximately 7-10 colonies of cells from each streak were harvested and counted.

Measuring cell sizes using the phase-contrast microscope

Cells from each senescence streak were scraped using a sterile toothpick into 500 µl ddH₂O in a 1.5 ml microfuge tube by propeller twisting the toothpick. This tube was considered the original stock solution and was vortexed for ~ 10 seconds. A 250 µl aliquot of cells from the original stock solution was further diluted 1:5 into 1000 µl ddH₂O in a new tube. The new diluted tube was vortexed for ~ 10 seconds and sonicated for 8 - 10 seconds. Then 12 µl – 16 µl of diluted cells were transferred on to the hemocytometer. The camera's image capture program, called ScopeImage DynamicPro, was used to visualize fields of cells and to overlay a distance scale over the field. The distances between the ticks (space) on the scale varied depending on the objective used.

The size of each cell was measured and was calculated by using the following formula relating the spaces between tick marks on the scale and distance in micrometers.

In the 40X Objective, 1 space = 2.5 μm

In the 100X Objective, 1 space = 1.1 μm or 0.72 μm (depending on the computer used)

Both unbudded and budded cells were analyzed. The sizes of the budded cells were measured by measuring the diameter of the mother cell. Cells that were picked for each measurement were moved so they were next to the scale before their sizes were determined. The widest diameter, either vertically or horizontally was picked for the measurement of the cell size. Between 10 and 20 cells were measured randomly and averages and standard deviations were calculated. For 100X measurements, 100% glycerol was placed onto the coverslip. A total of 12 μl – 16 μl of diluted cells were transferred onto the hemocytometer. Then, 50 μl of glycerol was added on the top of the coverslip to have a clear view of cells for the measurement.

Analysis of cell sedimentation rates using light scattering

Cells from each senescence streak were scraped from a plate and transferred into 500 μl ddH₂O in a 1.5 ml microfuge tube. This tube was considered the original stock solution and was vortexed for ~ 10 seconds. An aliquot of 25.6 μl of cells from the original stock solution was further diluted 1/40 in 1000 μl ddH₂O in a new 1.5 ml microfuge tube. The 1/40 diluted tube was vortexed and sonicated for ~ 15 seconds and 12 μl – 16 μl of the cells were transferred onto a hemocytometer. Cells were counted using the 40X objective to determine the required volume of cells needed to make new

solutions at concentrations of 1×10^6 cells/ml or 1×10^7 cells/ml or 1×10^8 cells/ml. X μ l of original stock solution was added to $1000\mu\text{l} - X \mu\text{l}$ of ddH₂O. Below is an example of the calculation for determination of the required volume of cells needed to make a 1×10^7 cells/ml suspension of cells.

For example:

If the average number of cells in each square of the 25-square grid on the hemocytometer is 11.33, then the cell titer is:

$$\begin{aligned} & 11.33 \times 25 \text{ squares} \times 10,000 \times 40 / 1 \\ & = 1.13 \times 10^8 \text{ cells/ml} \end{aligned}$$

To make a 1×10^7 cells/ml suspension, we need = $(1 \times 10^7 \text{ cells/ml}) / (1.13 \times 10^8 \text{ cells/ml})$

$$= 0.0885 \text{ ml}$$

$$= 88.5 \mu\text{l}$$

For a total volume of 1000 μ l,

88.5 μ l of cells from the original concentrated stock solution was added to 911.5 μ l ($1000 \mu\text{l} - 88.5 \mu\text{l}$) of ddH₂O to make the final concentration 1×10^7 cells/ml.

Two ml suspensions of cells at 1×10^7 cells/ml were made in 15 ml screwcap tubes. Cells were vortexed for ~ 10 seconds and sonicated for ~ 15 seconds in the 15 ml tube. Aliquots containing 450 μ l of sonicated cells were quickly transferred into 4 different cuvettes for measurement of the sedimentation rates of normal and senescent cells. The OD₆₀₀ was measured in a spectrophotometer for 70 minutes at 10 minute intervals. A cuvette containing 500 μ l ddH₂O was used as a blank and the OD₆₀₀ of 4

different samples of normal cells and senescent cells (Streak 1 – Streak 4) were then determined.

Gel electrophoresis

Horizon 11-14 gel rigs were used to perform gel electrophoresis using 0.7% - 0.9% agarose gels in 1 X TAE buffer (40 mM Tris, 20 mM acetic acid, 1 mM EDTA) at voltages of 100 V – 123 V. Gels were stained in ethidium bromide (0.5 µg/ml) for 15 – 20 minutes. Gel images were captured using an Alpha Innotech Red Imaging system.

E. coli plasmid DNA was prepared using a QIAprep Spin Miniprep Kit (Qiagen, Hilden, Germany) as described by the manufacturer. Plasmid DNAs were eluted in 50 µl of EB buffer.

PCR amplification

PCR reactions consisted of 2 µl of plasmid DNA, 1 µM A primer, 1 µM B primer, 0.25 mM dNTPs, 1X Thermopol buffer and 1 µl Taq polymerase (5 units) in a final volume of 50 µl. PCR reactions were run on a T100 Thermal Cycler with denaturation at 94°C for 30 seconds, annealing temperature of 51 - 52°C for 40 seconds and extension at 72°C for 1 minute (1 minute for the first 1000 bp with an addition of 30 seconds for each additional 1000 bp). The PCR product was confirmed using gel electrophoresis.

Purification / Ethanol Precipitation of PCR fragment DNA

PCR DNA products that produced a strong band were combined into one 1.5 ml microfuge tube and the total volume was calculated. Then 1/10 of the total volume of 3 M NaOAc was added, the solution was vortexed for ~ 2 seconds, and 2.5 volumes of cold 100% ethanol was added. The solution was vortexed and the tube was spun for 15 minutes at 21,000 x g. The supernatant was gently pulled off and discarded. Then 500 μ l of cold 70% ethanol was added gently to the pellet and it was re-spun for 3 minutes at 21,000 x g. The supernatant liquid was discarded and the tube was dried in a SpeedVac for 10 minutes. The pellet was resuspended in 1/5 of the original volume using ddH₂O.

Yeast transformations

Transformation of plasmid DNA or PCR fragment DNA into yeast cells was performed using the modified rapid transformation of early stationary phase yeast cells protocol of Tripp *et al.* (37). After the 42°C heat shock step, cells were spread initially onto non-selective YPDA plates and grown at 30°C for 1-2 days. The lawn formed after the transformation was replica plated by using double imprint replica plating to a YPDA plate using sterile velvets. Then, from that YPDA plate an imprint was made onto a YPDA + Nat (nourseothricin) plate using the same velvet. The reason for replica plating first on a YPDA plate was to reduce cell density and get clean colonies on the YPDA + Nat plate. The plate was incubated at 30°C for 2-3 days.

Chromosomal DNA purification

Colonies formed on YPDA + Nat plates after transformation were patched onto fresh YPDA + Nat plates. The patched plates were incubated at 30°C for 2 days. Colonies of cells from patched plates were taken for chromosomal DNA purification.

Chromosomal DNA purification was performed using the optimized protocol developed in the Lewis laboratory for the extraction of yeast chromosomal DNA (38). The purified chromosomal DNA was resolved using gel electrophoresis. Proper insertion of the Nat gene was verified through PCR using 5pdr5 and 3pdr5 test primers at 42°C annealing temperature for 40 seconds, extension at 72°C for 2 minutes and 45 seconds, and denaturing at 94°C for 30 seconds for 34 cycles. Again, the PCR product was then resolved using gel electrophoresis.

III. RESULTS AND DISCUSSION

The major goal of this project was to complete the development and testing of a new senescence assay. In Dr. Lewis laboratory, a yeast strain (YLKL803) has been developed for measuring the rate of cell aging. The strain has a plasmid (pLKL82Y), which contains the *EST2* polymerase gene under the control of a galactose-regulated promoter. When cells are grown in galactose media the *GALI-V10p* promoter is on and telomerase is expressed and cells are immortal (Figure 4). However, when cells are grown on glucose media the promoter is off and telomerase activity is halted. As a result the telomeres get shorter and shorter and eventually senescence occurs after $\sim 60 - 70$ generations (Figure 4, right side) (19, 29).

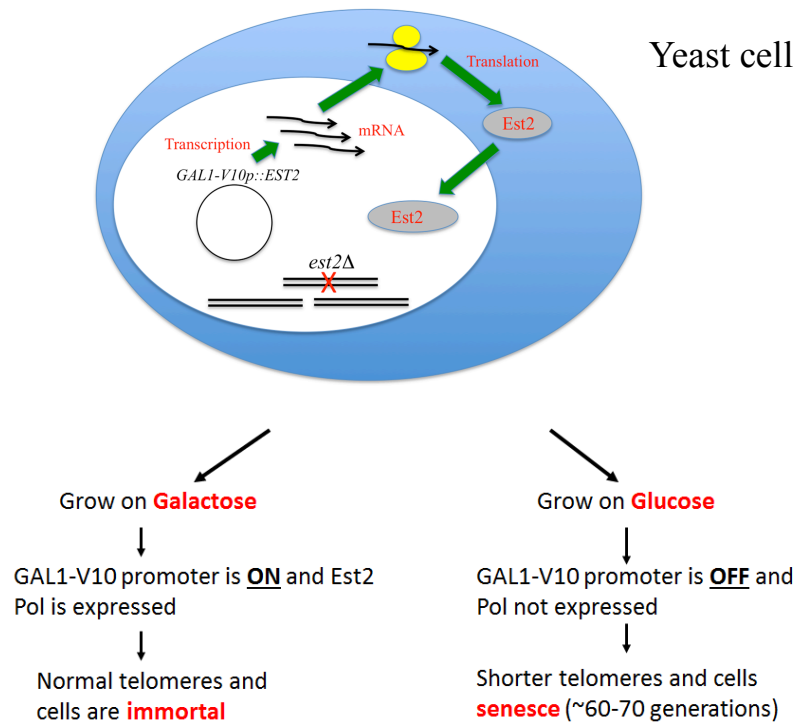


Figure 4. Diagram showing the yeast strain YLKL803 with a plasmid containing *EST2* polymerase under the control of a galactose regulated promoter. In the presence of galactose (left), cells have normal telomeres whereas in the presence of glucose (right), the cells have shorter telomeres.

Historically, senescence has been measured by growing telomerase-deficient cells on either rich or synthetic media plates with a series of four streaks of double columns. As shown in Figure 5, in previous senescence assays cells from a single colony were picked and streaked onto another plate and incubated at 30°C for 3-4 days to allow the single cells to form new colonies. For the second streak, a colony formed on the first streak plate was restreaked onto a new plate and incubated for 3-4 days at 30°C. The process was repeated for a third and a fourth streak. It was observed that wildtype cells could be streaked and restreaked indefinitely and never senesced due to the presence of

telomerase (Figure 5, left side). However, in telomerase-deficient cells, senescence was observed on the 4th streak, after > 60 generations or cell cycles (Figure 5, right side).

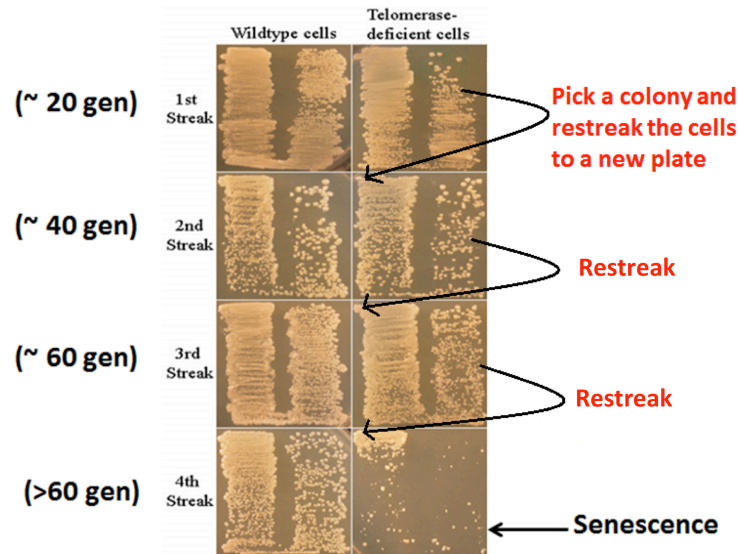
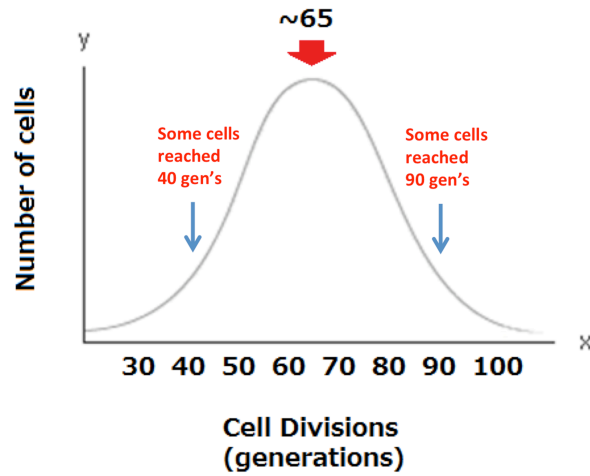


Figure 5. Diagram showing the historical method of streaking double columns of cells for solid media-based senescence assays.

Senescence is a stochastic process, meaning it is random. Most yeast cells normally stop growing after ~ 60 – 70 generations. However, in some cells, telomeres happen to get shorter faster than in other cells. Some cells only divide for ~ 40 cell cycles before they stop growing. In contrast, some yeast cells can go up to 90 generations before they undergo senescence (Figure 6A). Because of this random nature of senescence, there is considerable variability in the formation of colonies on the 4th streak (Figure 6B). Telomerase-deficient cells usually exhibit poor growth of colonies on the 4th streak plate, but the amount of growth differs from assay to assay, making quantitation difficult.

A



B

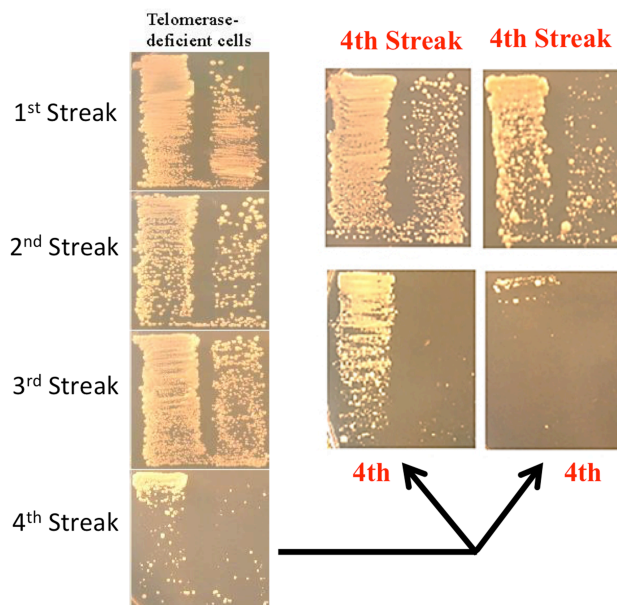


Figure 6. Diagram illustrating the stochastic process of senescence. (A) Most yeast cells senesce within ~ 65 generations. (B) The number of colonies that form on the 4th streak is reduced but highly variable. Images on the right side represent independent streaks of colonies from a 3rd streak plate to a 4th streak plate. Image source: Naoko Araki.

Naoko Araki and Neda Ghanem, former graduate students in the lab, developed a new statistics-based senescence assay in the Lewis lab (Figure 7) to improve the analysis of colonies on the 4th streak. This new assay has allowed measurement of aging quantitatively with strong statistics. In this assay, the first and second streaks were performed like the historical method (Figure 7, left side, showing 1st streak and 2nd streak). However, on the third and fourth streak plates, cells from single colonies were picked and streaked as single tall columns in a grid pattern using a printed template picture placed under the plate. On the third and fourth streaks, 48 separate tall columns were streaked out from 48 individual colonies onto 6 different plates (Figure 7, right side). The cells were incubated at 30°C for 3-4 days and the number of columns that achieved confluent (complete) growth was scored. Typically, almost all columns show full growth on the 3rd streak, but only approximately one-fourth of them are fully grown on the 4th streak plate due to senescence. This large number of individual column assays (48) has allowed measurement of the rate of senescence as the average number of full columns that form on the 4th streak plates.

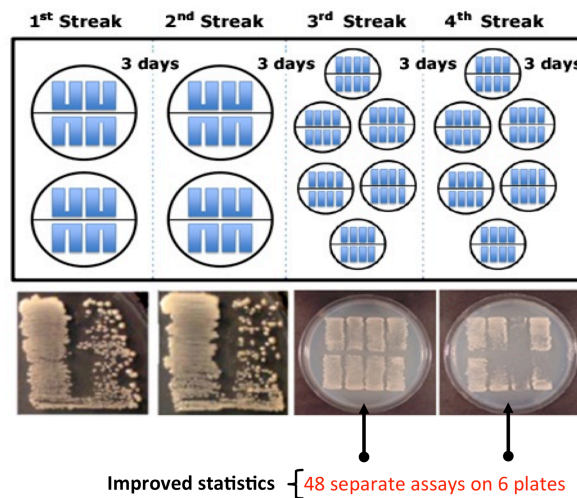


Figure 7. The new statistics-based senescence assay developed in this lab by Naoko Araki and Neda Ghanem (19, 29).

In addition to these improvements, another improvement made in the current study was to select more uniformly sized colonies for streaking than in past experiments. The diameter of each single colony that was picked for streaking was approximately 1/32 inch (0.8 mm) and these were selected in a consistent manner (Figure 9).

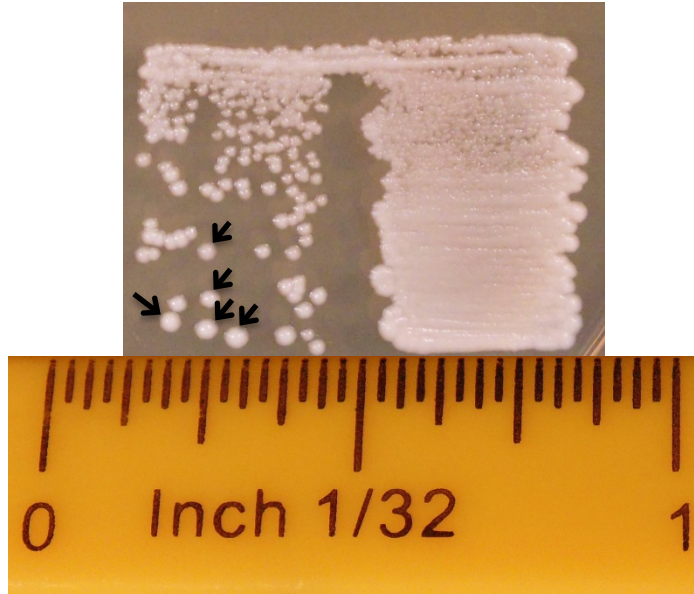
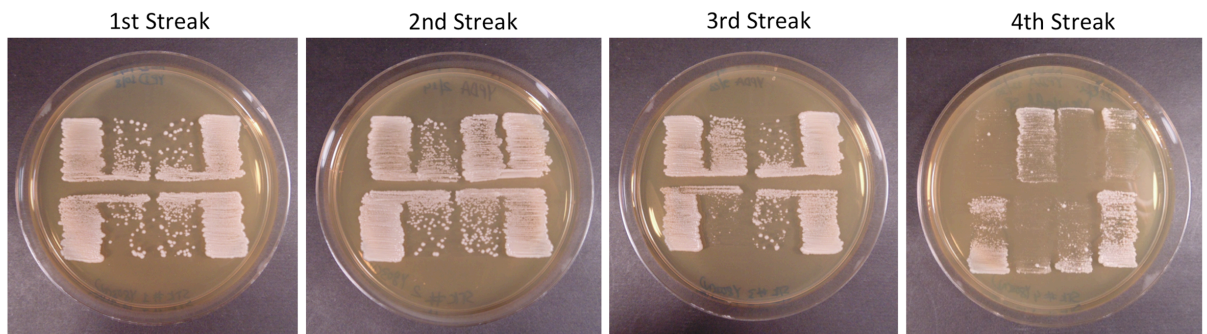


Figure 9. Diagram showing the typical size of a colony picked for each senescence cell streak. The diameter of each single colony was approximately 1/32 inch or 0.8 mm and this colony selection made the assays more consistent.

Figure 10 shows examples of plates generated using the improved senescence assay performed on rich media (YPDA) and synthetic media (glucose complete) in the current study. Note that only the 4th streak plates have tall columns of cells, while the 1st, 2nd and 3rd streak plates have “double columns”. Each 4th streak plate has 8 tall columns, each produced from a single colony on a 3rd streak plate. In this example, only one tall column on the YPDA 4th streak plate resulted in a full column of growth after 3 days (Figure 10A, far right). The other 7 columns were not full because most of the cells in the colonies they were streaked from had lost their growth potential due to senescence.

A



B

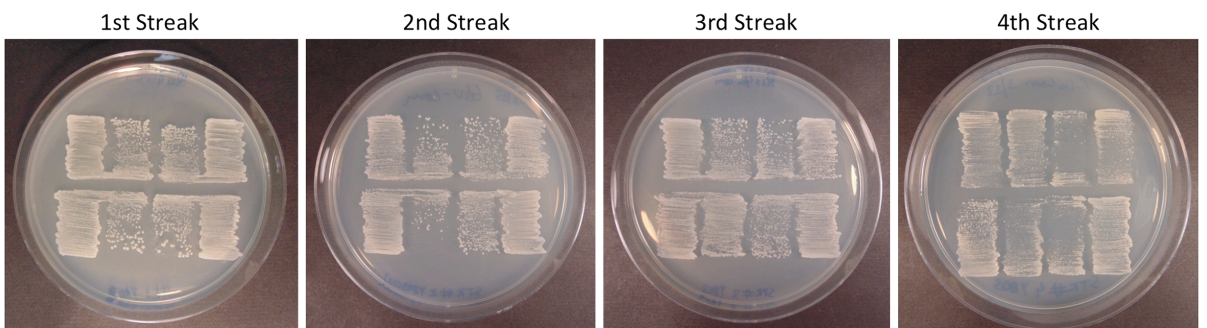


Figure 10. Examples of plate streaks performed for the new senescence assay. YLKL803 cells (*GAL1-V10p::EST2*) were streaked from galactose plates (*EST2* gene expressed) to glucose plates (*EST2* off) to initiate the first streak. All subsequent streaks were also on glucose plates. (A) Images of all the streaks performed on rich media (YPDA). (B) Images of all the streaks performed on synthetic media (glucose complete).

In past work, Neda Ghanem performed senescence assays using *est2* cells grown on rich YPDA media. In three separate trials, senescence was assessed on the 4th streak by measuring the total number of full columns on all plates and also the average number of full columns of growth out of 8 on each plate. In each of the trials only approximately 2 out of 8 columns on the plates were full columns (Table 4) (19).

Table 4. The number of full columns on the 4th streak of *est2* cells (YLKL803) grown on rich media in previous experiments. Adapted from (19).

	Full Columns	Average per Plate (#/8) (\pm SD)	Median
Trial 1	7/32	1.75 \pm 1.71	1.5
Trial 2	12/48	2.0 \pm 1.1	2.0
Trial 3	11/48	1.8 \pm 1.8	2.0

For the current project, two separate trials of senescence using *est2* cells (YLKL803) were also performed on rich media. The average number of full columns of growth per plate were 1.3 and 2.5 out of 8 columns (Table 5). This result is similar to the previous studies performed by Neda Ghanem, showing the reproducibility of the results. The total number of full columns, 8/48 and 15/48, were also similar to the results of Neda Ghanem.

Table 5. The number of full columns on the 4th streak of *est2* cells (YLKL803) grown on rich media performed for the current project.

	Full Columns	Average per Plate (#/8) (\pm SD)	Median
Trial 1	8/48	1.3 \pm 1.0	1.0
Trial 2	15/48	2.5 \pm 1.9	2.5

Initial experiments for this project worked to improve the assay system using YLKL803, in which telomerase expression was controlled by switching between galactose and glucose media. In the next experiment, another yeast strain (YLKL961) containing the pVL715 plasmid was tested. pVL715 has the *EST2* polymerase gene constitutively expressed from a moderately strong *ADHI* promoter and also has the *URA3* gene for selection (39) (Figure 11). This is another approach to determine the rate of senescence, where the promoter is not regulated by galactose.

Figure 11 is a schematic diagram illustrating this alternative method for conducting senescence assays. In this assay system, the strain YLKL961 was grown on a glucose minus uracil (Glu-ura) plate so that approximately all cells have the pVL715 plasmid containing the *EST2* polymerase gene, and therefore all cells have long telomeres initially. For the first streak of the assay, a colony was taken from the Glu-ura plate and streaked onto a 5-FOA plate. Plates containing the chemical 5-FOA (5-fluoroorotic acid) in them allow the growth of *ura3* mutant cells but not wildtype *URA3* cells. This is because *URA3* cells produce Ura3 enzyme, which acts on 5-FOA to make a toxic fluorinated byproduct that is lethal to cells. Thus, only cells that do not make Ura3

enzyme can survive on plates containing 5-FOA. If the *URA3* gene is on a plasmid, then only cells that have randomly lost the plasmid (about 1 in 10^3 - 10^4 cells during normal growth) can grow on 5-FOA plates. Because these cells have lost the plasmid, they are also now telomerase-deficient because *EST2* was on the plasmid. Four separate double columns were generated on the first streak to a 5-FOA plate and cells were incubated for 4 days at 30°C. On the 5-FOA plate only plasmidless cells grew up. Cells present on the first streak now lack the *EST2* polymerase gene and do not produce telomerase. For the second streak, colonies were picked from the 5-FOA plate and streaked on to a fresh glucose complete (synthetic complete media containing 2% glucose) plate. Cells were allowed to grow for 4 days at 30°C. For the third streak, single colonies from the second streak were picked and streaked onto a fresh plate as before. Finally, for the fourth streak, 48 different individual colonies were picked and streaked as tall single columns onto 6 different plates with the grid pattern template under the plate. On each plate, 8 separate individual columns were created as in the YLKL803 senescence assays (Figure 8 and Figure 10). Cells were allowed to grow for 3-4 days at 30°C.

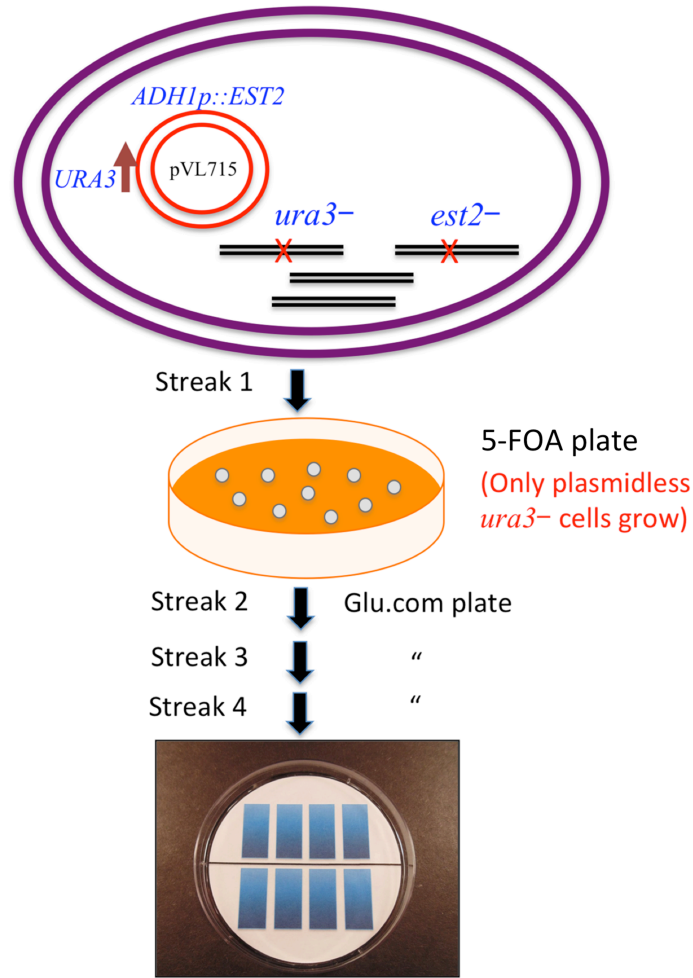


Figure 11. Schematic diagram illustrating an alternative method for conducting senescence assays. Senescence assays were designed to use pVL715 (*URA3 ADH1p::EST2*) and 5-FOA plates.

In this new assay, senescence was observed on the 4th streak as before. The number of full columns per plate was low, only 3.3 full columns out of 8 (Table 6). These results are similar to those obtained using YLKL803 and switching cells from galactose to glucose (Table 4 and Table 5).

Table 6. The number of full columns of growth on the 4th streak of *est2* cells (YLKL961) containing pVL715.

	Full Columns	Average per Plate (#/8) (\pm SD)	Median
Streak 4	20/48	3.3 \pm 1.5	3.0

The goal of the next experiment was to calculate the number of generations (cell divisions) undergone by the senescing cells before they stopped dividing. It is believed that telomerase-deficient cells can divide about 60-70 times before ceasing growth, but this is not easy to quantitate. In the past, experiments involving counting the number of generations of growth within colonies on senescence streak plates (19) were performed by Neda Ghanem. That work used long 9 inch Pasteur pipettes to harvest entire single colonies from a plate surface. After coring each colony with a Pasteur pipette, the agar plug plus cells were transferred into a microfuge tube containing 500 μ l ddH₂O. Cells were vortexed hard for \sim 10 seconds, sonicated for 10 seconds, then counted on a hemocytometer using a phase contrast microscope (19). After determining the total number of cells in a colony, the number of generations that the cell went through was calculated. After being streaked to a plate surface, 1 cell divides into 2 cells and 2 cells into 4 cells and so on multiple times to form a single colony of more than a million cells (depicted schematically in Figure 12). The total number of cells present in a single colony can be calculated by using the following formula:

2^y = total number of cells in a colony, where y = the number of cell divisions that cells went through to form the colony.

For example, a colony of 4 cells has undergone 2 divisions (2^2) and a colony of 8 cells has undergone 3 divisions (2^3). Table 7 shows the total number of cells per colony after several generations of growth. For example, there are 2,097,152 cells in a colony that has undergone exactly 21 cell divisions.

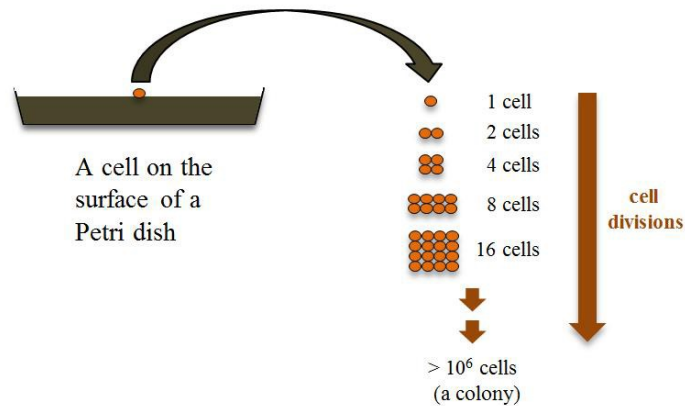


Figure 12. Diagram showing multiple divisions of a single cell to form a colony.

Table 7. The total number of cells in a single colony for each generation of growth.

Number of generations	Total number of cells per colony
1 st generation	2
2 nd generation	4
.	.
.	.
.	.
15 th generation	32,768
16 th generation	65,536
17 th generation	131,072
18 th generations	262,144
19 th generation	524,288
20 th generation	1,048,576
21 st generation	2,097,152

In following up on the previous work, I noticed that the diameter of the Pasteur pipette was sometimes equal to or smaller than the diameter of the colony being cored and thus sometimes not all of the cells were harvested from the colony. I also observed that a fraction of the cells were sticking to the walls of the Pasteur pipette and that pipetting up and down in water was necessary to get all of the cells out of the pipette. To solve the problem caused by the small diameter of the Pasteur pipette, I determined that use of a long 1 ml plastic pipette of the kind normally used in conjunction with an electronic pipettor could improve the method. The opening at the end of this pipette has a larger diameter (bore size) that can accommodate larger colonies. Also, the long pipette can be attached to an electronic pipettor (or pipet aid) and used to pull a whole colony up into the pipette via vacuum pressure (Figure 13).

An experiment was designed to count the number of generations that cells went through to form a colony during senescence. As shown in Figure 13, a 1 ml plastic pipette with an attached electronic pipette aid was used to harvest cells from a single colony. The pipette aid was used to pull the colony with agar from the Petri dish as shown in Figure 13B and 13C. Then the colony with the plug of agar was transferred into a microfuge tube containing 500 μ l or 1000 μ l ddH₂O. The 1 ml plastic pipette was rinsed 3-4 times with ddH₂O from the recipient tube. The cells were vortexed hard for ~ 10 seconds to separate cells from the agar and cells were then sonicated for 10 seconds. Approximately 12 μ l – 16 μ l of cells were then quickly transferred on to a hemocytometer and cells were counted using a phase contrast microscope.

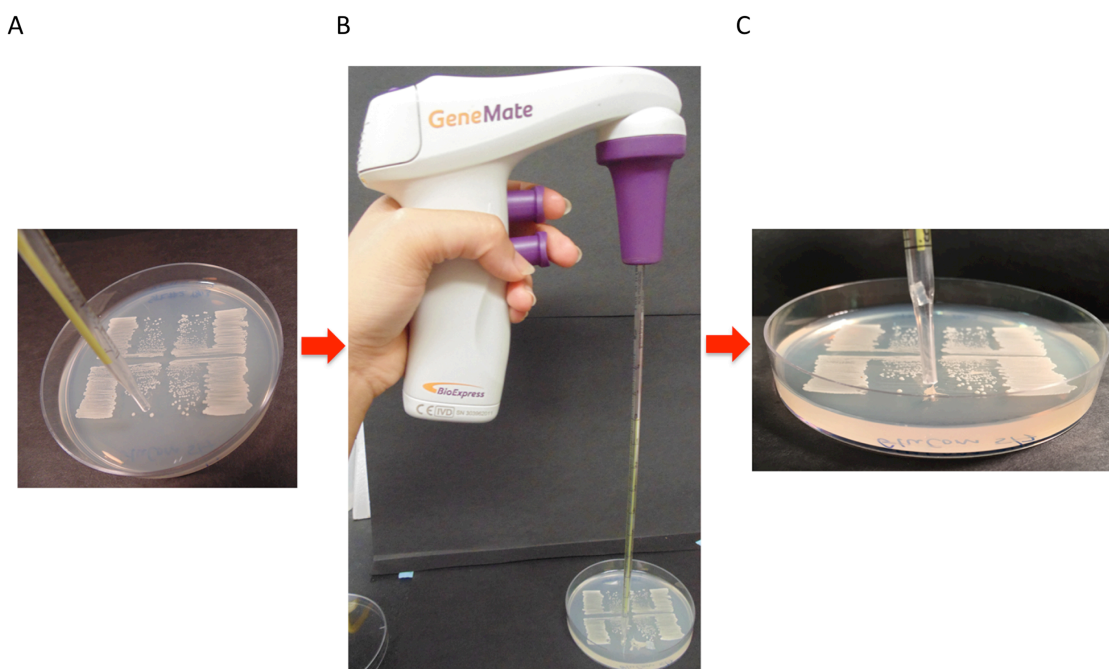


Figure 13. New method using 1 ml plastic pipette with an attached electronic pipet aid to core colonies. (A) 1 ml plastic pipette was held vertically onto the colony and pushed until the plastic pipette reached the bottom of the plate. (B) The pipet aid was used to pull the colony with agar from the petri dish. (C) A colony and its agar plug are shown inside a 1 ml plastic pipette.

Both long 9 inch Pasteur pipettes and 1 ml plastic pipettes were used separately to calculate the number of generations that cells went through to form colonies during senescence on rich media. Approximately 7-10 colonies of cells from each streak were harvested and counted. The results are shown in Table 8 and Table 9. When 9 inch Pasteur pipettes were used to harvest all the cells from a colony the number of generations undergone by *est2* cells on the 1st, 2nd and after 3rd streaks was determined to be 57.4 on rich media (Table 8). When the same experiment was performed using the larger bore 1 ml plastic pipette the number of generations was calculated to be 63.3

(Table 9). This increase in the calculated cells per colony and number of cell divisions is a clear indication that the smaller diameter of the Pasteur pipette resulted in capture of fewer cells. These results show the advantages of using a 1 ml plastic pipette for quantitative determination of the number of generations accurately.

Table 8: The number of generations that cells went through during each streak of *est2* cells on rich media using a Pasteur pipette.

	Average number of cells per colony	Number of generations (\pm SD)
Streak 1	1.2×10^6	20.1 ± 0.4
Streak 2	1.1×10^6	20.0 ± 0.3
Streak 3	0.2×10^6	17.3 ± 0.8
Total generations		57.4

Table 9: The number of generations that cells went through during each streak of *est2* cells on rich media using a 1 ml plastic pipette.

	Average number of cells per colony	Number of generations (\pm SD)
Streak 1	3.0×10^6	21.4 ± 0.4
Streak 2	3.4×10^6	21.6 ± 0.3
Streak 3	1.4×10^6	20.3 ± 0.4
Total generations		63.3

A similar experiment was performed with *est2* cells grown on synthetic media (rather than rich YPDA media) using either a 1 ml plastic pipette or a long 9 inch Pasteur pipette. The results are shown in Tables 10 and 11. The number of generations calculated using 1 ml plastic pipettes was 64.7 generations, which is higher than the 57.0 generations calculated using Pasteur pipettes. Results with the 1 ml plastic pipette indicate that cells are undergoing 63-65 cells divisions in the senescence experiments employed for this project during the first 3 streaks. This is a minimum number because many of the cells undergo a small number of divisions on the 4th streak plate before losing their capacity for growth.

Table 10: The number of generations that cells went through during each streak of *est2* cells on synthetic media using a Pasteur pipette.

	Average number of cells per colony	Number of generations (\pm SD)
Streak 1	0.5×10^6	18.9 ± 0.6
Streak 2	0.6×10^6	19.2 ± 0.5
Streak 3	0.5×10^6	18.9 ± 0.7
Total generations		57.0

Table 11: The number of generations that cells went through during each streak of *est2* cells on synthetic media using a 1 ml plastic pipette.

	Average number of cells per colony	Number of generations (\pm SD)
Streak 1	3.4×10^6	21.6 ± 0.3
Streak 2	4.4×10^6	22.0 ± 0.4
Streak 3	2.4×10^6	21.1 ± 0.3
Total generations		64.7

Yeast cells with *RAD52* knocked out are defective in homologous recombination. When telomerase is also inactivated, e.g. in *rad52 est2* double mutant cells, senescence is accelerated (16, 19). While *est2* cells undergo ~ 60 – 70 cell divisions and senesce on the 4th streak plate, *rad52 est2* cells undergo only ~ 40 divisions and exhibit senescence on the 3rd streak plate. Experiments were performed with *est2 rad52* (YCLK807) cells on rich and synthetic media using 1 ml plastic pipettes. The number of generations of growth undergone during each of the streaks is shown in Tables 12 and 13. *est2 rad52* cells displayed a low number of total generations on rich media (42.3) and on synthetic media (42.7).

Table 12: The number of generations that cells went through during each streak of *est2 rad 52* cells on rich media using a 1 ml plastic pipette.

	Average number of cells per colony	Number of generations (\pm SD)
Streak 1	3.9×10^6	21.8 ± 0.6
Streak 2	1.5×10^6	20.5 ± 0.8
Total generations		42.3

Table 13: The number of generations that cells went through during each streak of *est2 rad 52* cells on synthetic media using a 1 ml plastic pipette.

	Average number of cells per colony	Number of generations (\pm SD)
Streak 1	3.0×10^6	21.4 ± 0.3
Streak 2	2.8×10^6	21.3 ± 0.2
Total generations		42.7

The next major goal of this project was to measure changes in cell morphology during aging. Past studies of yeast cell senescence have noted that, during aging, cells appeared to become enlarged as telomeres got shorter (Figure 14) (16, 18, 20). However, the magnitudes of these changes have never been quantitated before.

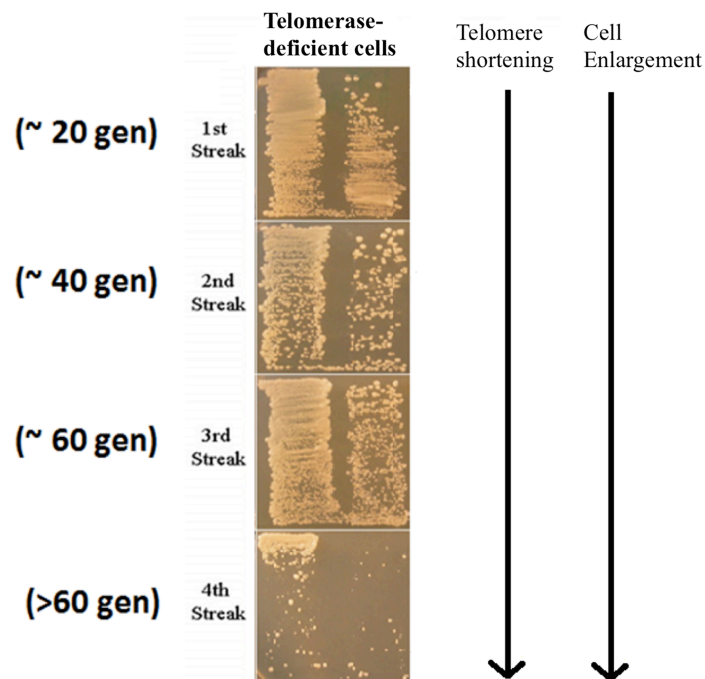
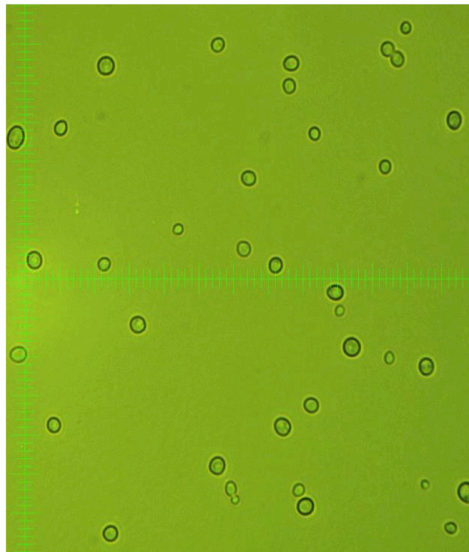


Figure 14. Cells increase in size during senescence, but the magnitudes of these changes have never been measured (16, 18, 20).

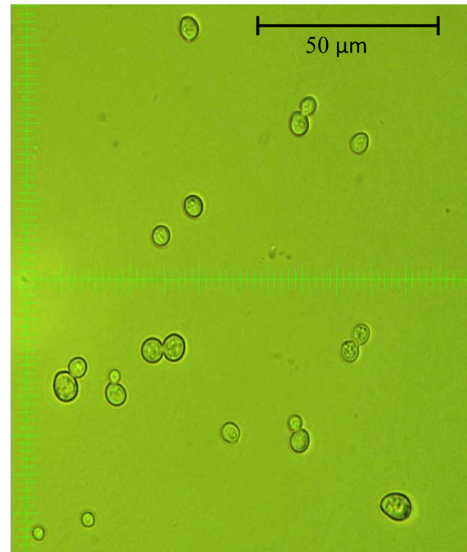
In this study a video camera-linked phase contrast microscope was used to measure the sizes of normal cells and senescent cells after each of the streaks (1st, 2nd, 3rd and 4th) at both 400X and 1000X magnification.

Figure 15 shows a comparison between normal and senescent cells (taken from a 4th streak plate). Normal cells are much smaller compared to senescent cells. For each of the experiments performed below a software-generated scale was used to measure the diameters of unbudded and budded cells as described earlier in the Materials and Methods chapter. Between 10 and 20 cells were measured randomly and averages and standard deviations were calculated.



Normal Cells

- Small
- Mostly G1 phase



Senescent cells

- Large
- Many G2 phase cells

Figure 15. Comparison of normal and senescent cells. Normal cells are smaller in size as compared to senescent cells. Wildtype cells and senescent 4th streak plate cells were harvested, sonicated and visualized using phase contrast microscopy. Magnification: 400X

Normal (*EST2*) cells were compared to completely senescent 4th streak *est2* cells on YPDA media initially. Sizes of unbudded (G₁ phase) cells were counted separately from budded cells, which may be in S, G₂ or M phase. This was done to try to detect cell cycle phase-specific changes during senescence. Unbudded normal cells had an average diameter of 5.4 μ m (Figure 16A and 16B). In contrast, unbudded senescent cells had an average diameter of 8.2 μ m, an increase of 51.9%

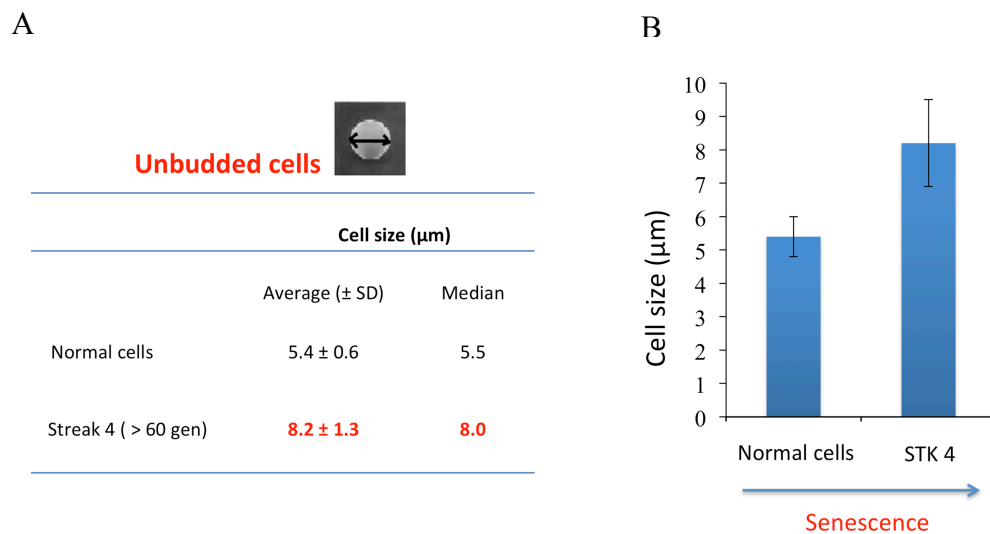



Figure 16. Measurement of the sizes of normal and senescent (4th streak) unbudded cells on rich media (YPDA) using the phase contrast microscope with a 40X objective (400X magnification). STK 4, senescence streak number 4. (A) Mean and median cell sizes. (B) Graph showing average sizes. Error bars indicate standard deviations.

In the assay shown in Figure 17, the diameters of unbudded *est2* cells from each of the streaks on rich media were assessed using 400X magnification as before. The average sizes of the cells after each of the streaks increased linearly during senescence, changing from 5.3 μ m after the 1st streak (~20 generations) to 8.2 μ m after the 4th streak.

A

Unbudded cells 

	Cell size (μm)	
	Average (\pm SD)	Median
Normal cells	5.4 ± 0.6	5.5
Streak 1 (~ 20 gen)	5.3 ± 1.1	5.0
Streak 2 (~ 40 gen)	6.6 ± 1.0	7.0
Streak 3 (~ 60 gen)	7.3 ± 1.7	7.0
Streak 4 (> 60 gen)	8.2 ± 1.3	8.0

B

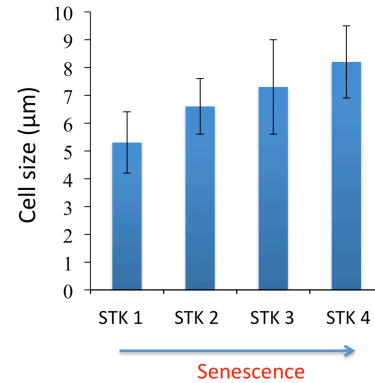
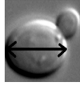


Figure 17. Measurement of the sizes of unbudded cells after each streak on rich media (YPDA) using the phase contrast microscope with 400X magnification. (A) Mean and median cell sizes. (B) Graph showing average sizes after each streak.

A similar experiment was performed next on budded cells. The wildtype budded cells had an average size of $6.3 \mu\text{m}$ and this increased to $10.1 \mu\text{m}$ in fully senescent cells (Figure 18). Thus, the average size of the senescent cells was increased by 60.3%. Here also there was a nearly linear increase of average size among budded cells after each of the streaks (Figure 19).

A

Budded cells



	Cell size (μm)	
	Average (\pm SD)	Median
Normal cells	6.3 \pm 0.7	6.3
Streak 4 (> 60 gen)	10.1 \pm 1.6	10.0

B

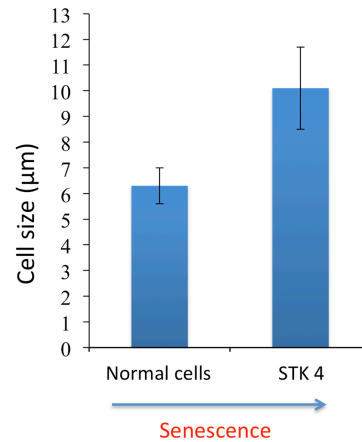
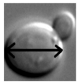


Figure 18. Measurement of the sizes of wildtype and senescent (4th streak) budded cells on rich media (YPDA) using 400X magnification. (A) Mean and median cell sizes. (B) Graph showing average sizes.

A

Budded cells



	Cell size (μm)	
	Average (\pm SD)	Median
Normal cells	6.3 \pm 0.7	6.3
Streak 1 (~ 20 gen)	6.5 \pm 1.6	6.0
Streak 2 (~ 40 gen)	6.7 \pm 1.4	7.3
Streak 3 (~ 60 gen)	8.3 \pm 1.3	8.8
Streak 4 (> 60 gen)	10.1 \pm 1.6	10.0

B

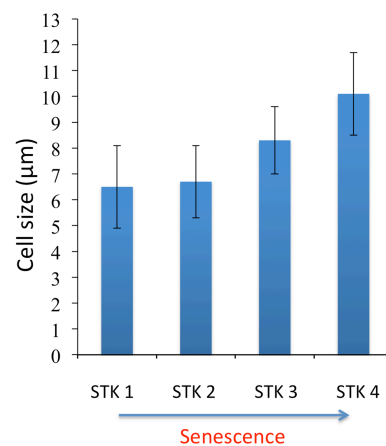


Figure 19. Measurement of the sizes of budded cells after each streak on rich media (YPDA) at 400X magnification. (A) Mean and median cell sizes. (B) Graph showing changes in average size after each streak.

Use of 1000X magnification on a phase contrast microscope requires use of an oil immersion objective (100X) and is therefore more difficult technically than lower magnifications. After some experimentation, conditions were developed involving immersion of the 100X objective into 100% glycerol that produced good images. These conditions were then used to employ 1000X magnification for measuring the diameters of unbudded and budded *est2* cells. Yeast cells appear much larger using the 100X objective than with the 40X objective. Figure 20 shows a representative image of normal and senescent cells alongside a green-colored scale used to measure the diameters of the unbudded and budded cells. Note that the cells appear much larger than in the 400X pictures in Figure 15 and therefore cell size measurements may be more accurate.

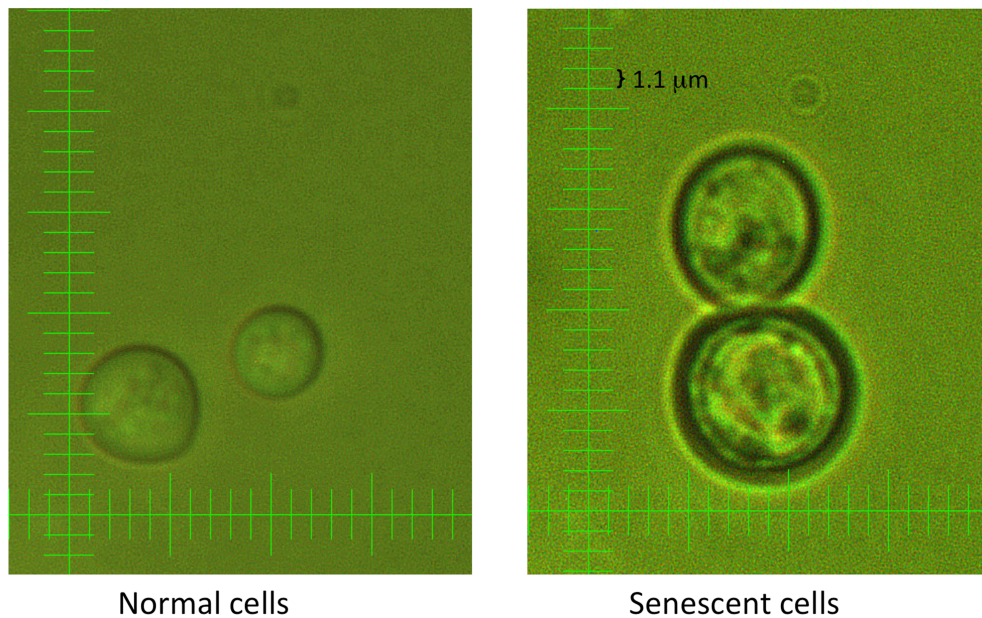


Figure 20. Yeast cells appear larger using a 100X objective than with a 40X objective. Images captured by camera using ScopeImage DynamicPro software showing the scale used to measure the diameter of the unbudded and budded cells with a 100X objective (1000X magnification). The distance between ticks on the scale is 1.1 μm

Using 1000X magnification and YLKL803 cells grown on rich YPDA media, unbudded cell sizes increased by 31.5% during senescence, increasing from an average size of 5.4 μm to 7.1 μm using 1000X magnification (Figure 21). Measurement of cell sizes after each streak indicated increases in average diameters from 5.5 μm on the 1st streak to 7.1 μm on the 4th streak (Figure 22).

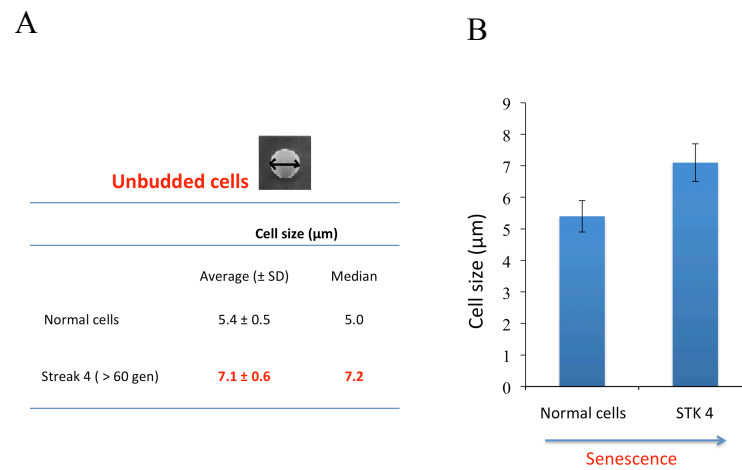


Figure 21. Measurement of the sizes of wildtype and senescent (4th streak) unbudded cells on rich media (YPDA) using 1000X magnification. (A) Mean and median cells sizes. (B) Plot of average sizes with standard deviations.

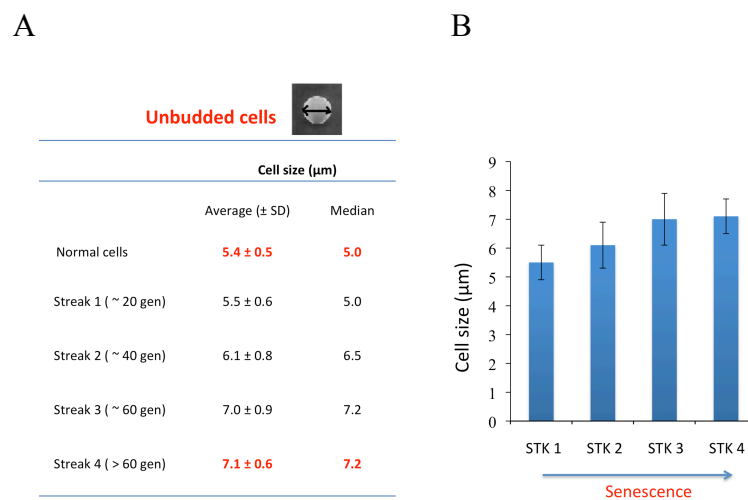


Figure 22. Measurement of the sizes of unbudded cells after each streak on rich media (YPDA) using 1000X magnification. (A) Mean and median cell sizes. (B) Plot of average cell sizes after 1st, 2nd, 3rd and 4th streaks.

In the case of budded cells, the average size increased by 15.9%, from 6.3 μm for normal cells to 7.3 μm for 4th streak cells when 1000X magnification was used. There was not much change in size during each of the streaks (Figure 23 and 24). This is different from the results seen at 400X magnification and it is not clear why the progressive increase after each streak was no longer present.

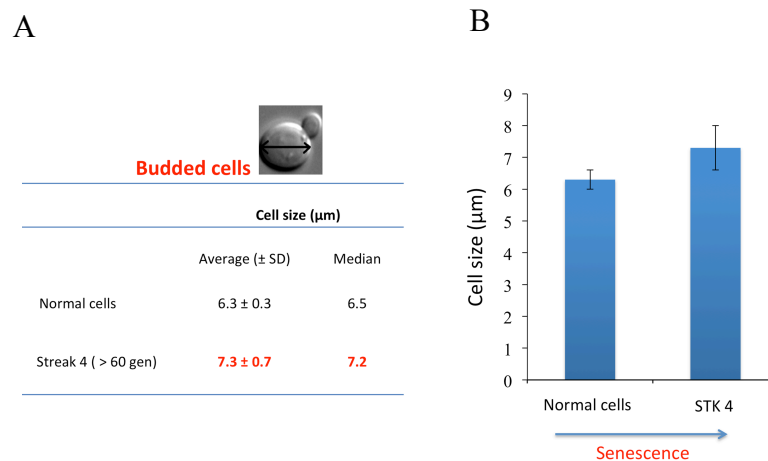


Figure 23. Measurement of the sizes of wildtype and senescent (4th streak) budded cells on rich media (YPDA) using 1000X magnification. (A) Mean and median sizes. (B) Graph showing average sizes and standard deviations.

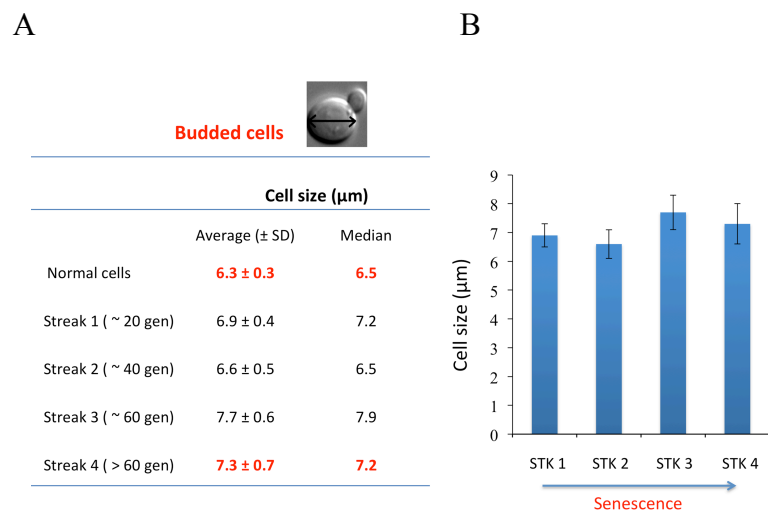


Figure 24. Measurement of the sizes of budded cells after each streak on rich media (YPDA) using 1000X magnifications. (A). Mean and median sizes. (B) Graph depicting changes in average size after each streak.

Using 1000X magnification and synthetic plates (glucose complete media), the unbudded cells' average size was increased by 39.7% during senescence, increasing from 5.8 μm to 8.1 μm in diameter (Figure 25). A comparison of unbudded cell sizes after each streak revealed an increase over time, from 6.4 μm after the 1st streak to 8.1 μm after the 4th streak (Figure 26).

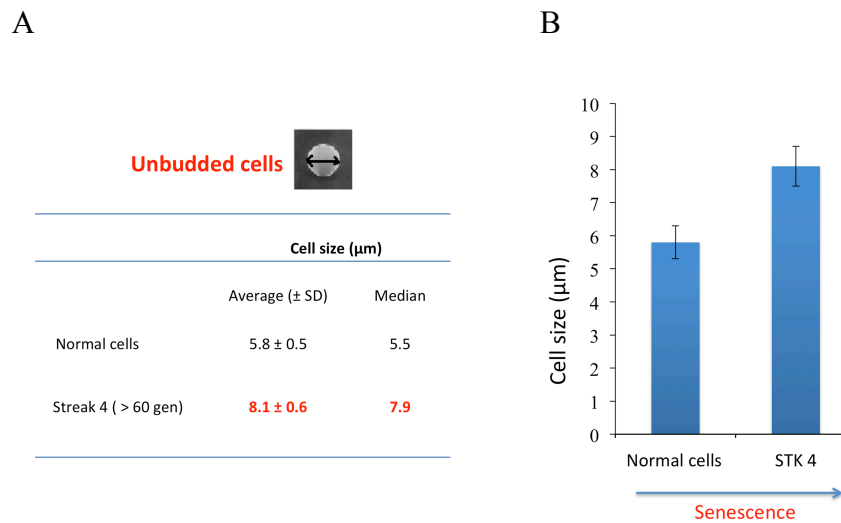


Figure 25. Measurement of the sizes of normal and senescent (4th streak) unbudded cells on synthetic media (glucose complete) using 1000X magnification. (A) Mean and median sizes. (B) Graph showing average sizes.

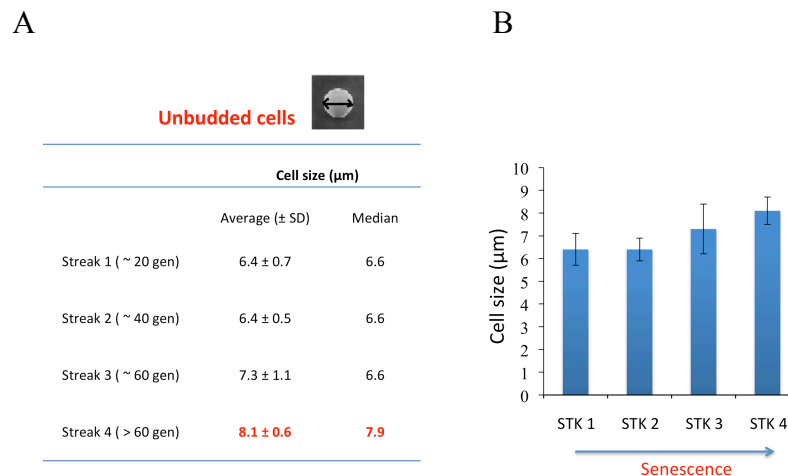


Figure 26. Measurement of the sizes of unbudded cells after each streak on synthetic media (glucose complete) using 1000X magnification. (A) Mean and median sizes. (B) Graph showing changes in average size after each streak.

At 1000X magnification and using synthetic plates, budded cells' average size was increased by 58.6% during senescence, changing from 5.8 μm for normal cells to 8.1 μm in diameter (Figure 27). Sizes increases were not strongly linear when 1st, 2nd, 3rd and 4th streak plates were compared, through sizes increased from 6.6 μm (1st streak) to 9.2 μm (4th streak) (Figure 28).

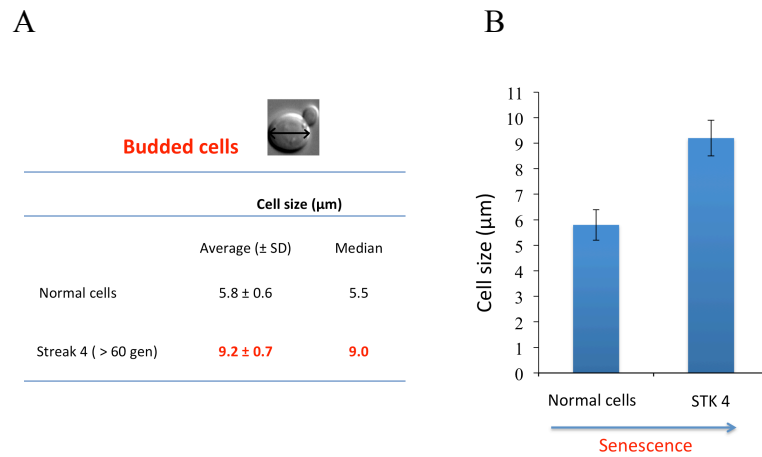


Figure 27. Measurement of the sizes of normal and senescent (4th streak) budded cells on synthetic media (glucose complete) at 1000X magnification. (A) Mean and median sizes. (B) Graph showing average sizes.

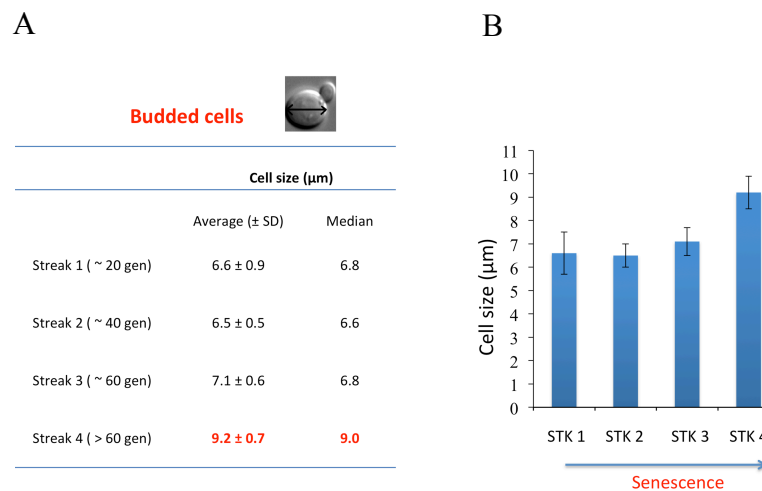


Figure 28. Measurement of the sizes of budded cells after each streak on synthetic media (glucose complete) using 1000X magnification. (A) Mean and median sizes. (B) Graph showing changes in average size after each streak.

Past studies have shown that the *RAD52* group of genes plays an important role in maintaining the lengths of telomeres through homologous recombination (16, 19, 28). Figure 29A shows genetic exchange between a long telomere and a short telomere, in which short telomere length got increased (discussed in Chapter I). Past studies performed in our lab revealed that *est2 rad52* cells senesce earlier, on the 3rd streak, than *est2* cells (which show senescence on the 4th streak) indicating the importance of *RAD52* gene in maintenance of telomere lengths (16).

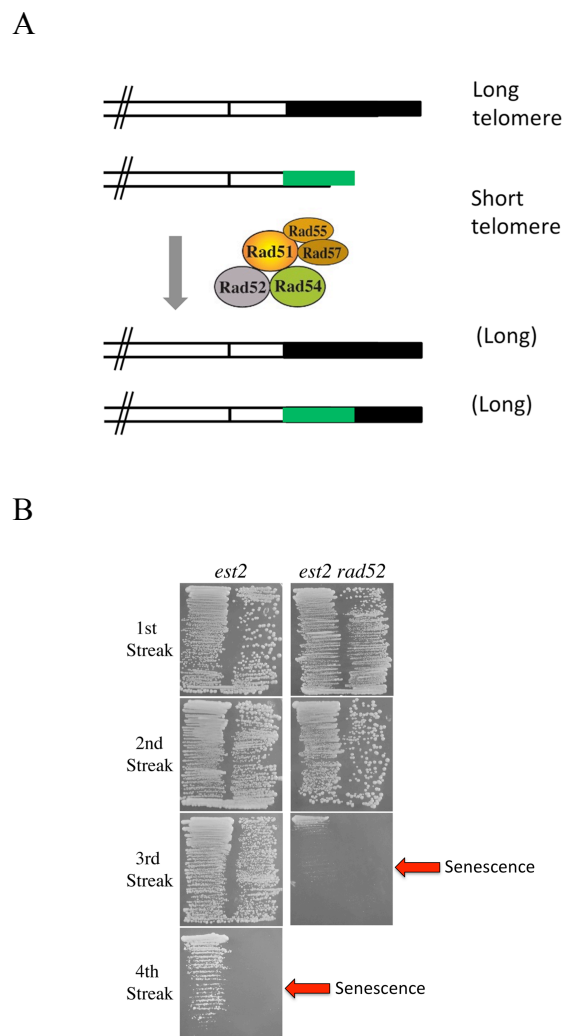


Figure 29. In *est2 rad52* cells, senescence occurs on the 3rd streak rather than on the 4th streak (16). (A) The schematic diagram showing homologous recombination between long and short telomere. (B) Plate picture showing the senescence of *est2* cells and *est2 rad52* cells. Source: Sandra Becerra.

The diameters of *est2 rad52* cells from each of the streaks on rich media were measured using 1000X magnification. The average size of normal *rad52* cells increased by 17.1% during senescence, from 8.2 μm to 9.6 μm (Figure 30A). However, the average size difference between each of the streaks of *est2 rad52* cells was small (Figure 30B). This may be because *est2 rad52* cells are comparatively bigger in size already in the first streak than *est2* cells. The average sizes of normal non-senescent cells was approximately 6 μm , whereas it was about 8.2 μm for non-senescent *rad52* cells. The *rad52 est2* cells were analyzed in more detail in Figure 31. Unbudded (G_1 phase), small budded (S phase), and large-budded (G_2/M) cells were analyzed separately to determine if there were cell cycle phase differences. Unbudded and large-budded cells showed the largest percent increases. As shown in Table 14, the average sizes of cells were increased by 25.3%, 4.6% and 24.1% in unbudded, small-budded and large-budded cells, respectively, during senescence.

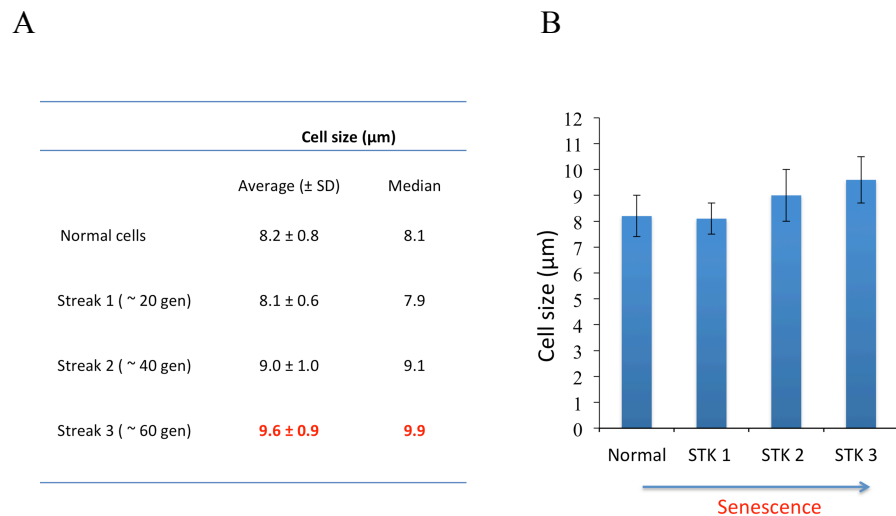


Figure 30. Measurement of the sizes of normal and senescent (4th streak) cells on rich media (YPDA) using 1000X magnification. The figure shows the average of all cells types (unbudded and budded). (A) Mean and median sizes. (B) Graph showing changes in average size after each streak.

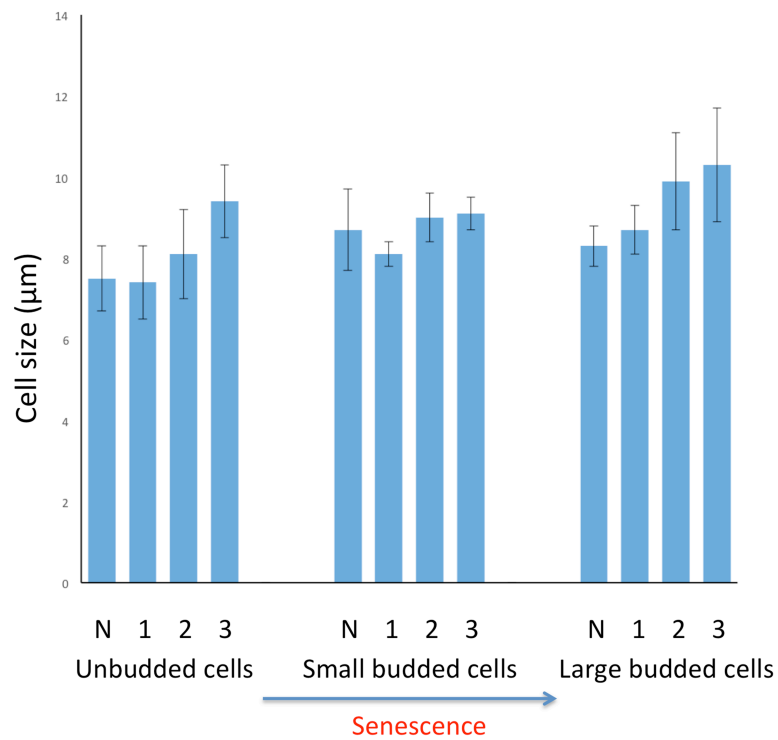


Figure 31. Measurement of the sizes of normal and senescent (4th streak) cells of all kinds on rich media (YPDA) using 1000X magnification.

Table 14: Percent change in sizes of *est2 rad52* cells on rich YPDA media measured using 1000 X magnification.

Cell type	Normal vs. Streak 3 (% change)
Unbudded	25.3
Small budded	4.6
Large budded	24.1

The next major goal of my project was to analyze how rates of sedimentation of cells change during senescence using light scattering and spectrophotometry. We formulated a hypothesis: if senescent cells are larger than normal cells, they may settle out of solution faster (depicted schematically in Figure 32). Cells suspended in solution can scatter light and we used this to analyze sedimentation of the cells. Before analyzing sedimentation, we first asked a simple question: do senescent cells exhibit greater light scattering than normal cells when they are at the same cell titer (number of cells per ml).

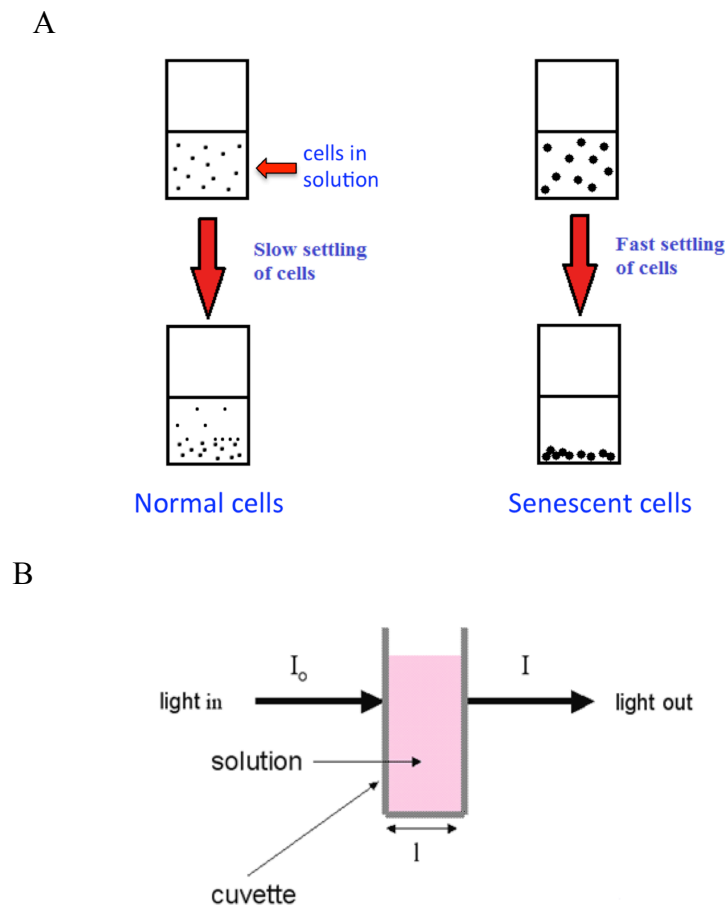


Figure 32. Schematic illustration of sedimentation of normal and senescent cells. (A) Diagram showing how senescent cells are larger than normal cells and may settle out of solution faster. (B) Diagram showing the spectrophotometric analysis of light scattering.

The OD₆₀₀ of multiple solutions of wildtype and senescent cells were measured at a titer of 1 X 10⁶ cells/ml and then separately at a titer of 1 X 10⁷ cells/ml. The senescent cells exhibited a higher average OD₆₀₀ (light scattering) than wildtype cells. As shown in Figure 33, the OD₆₀₀ of senescent cells was 21% and 32.6% higher than normal cells at 1 X 10⁶ cells/ml and 1 X 10⁷ cells/ml, respectively, indicating that there are modest differences in optical properties between the cells. This is likely to be due to the much larger size of the senescent cells and the fact that there are more large-budded cells among the senescent cells.

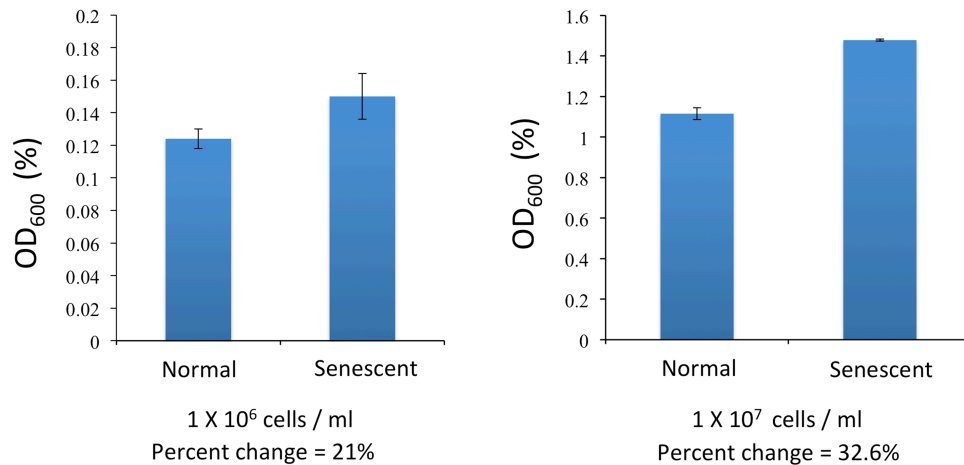
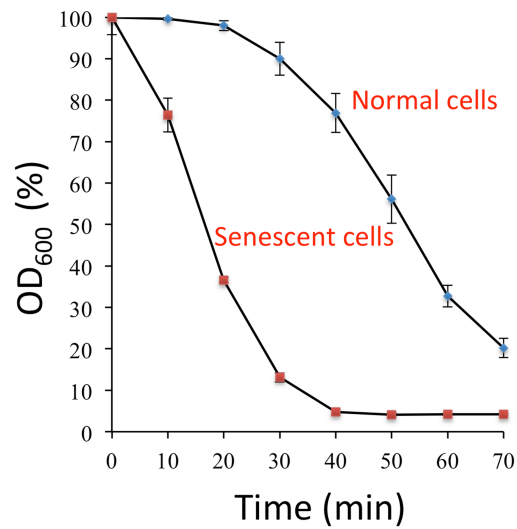


Figure 33. Senescent (*est2*) cells exhibit higher OD₆₀₀ values than wildtype cells. Normal and senescent cells were analyzed at titers of 1 X 10⁶ cells/ml or 1 X 10⁷ cells/ml.

The next experiment was set up to measure changes in the OD₆₀₀ of normal cells and *est2* cells from each of the four streaks at a cell titer of 1 X 10⁷ cells/ml measured over 70 minutes using 10 minute intervals. Senescent cells harvested from rich YPDA plates sedimented much more rapidly than normal cells. As shown in Figure 34A, 90% of senescent cells fell out of solution within 30 minutes, while only 10% of normal cells

were sedimented at that time. Figure 34B shows the sedimentation of each of the streaks of senescing cells on rich media. The results show a trend toward faster sedimentation after each streak.

A



B

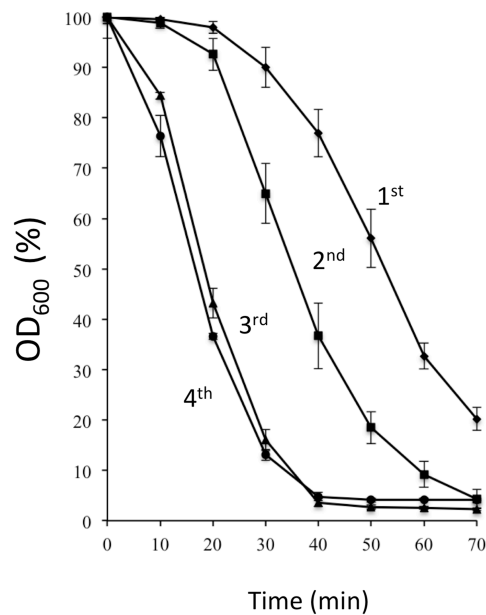
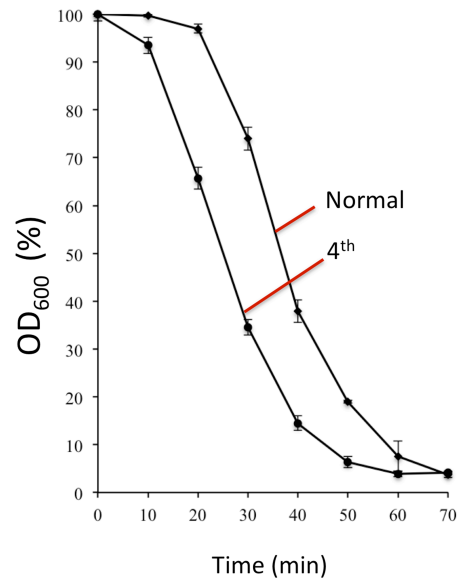


Figure 34. Older cells sediment more rapidly than normal cells. (A) Light scattering produced by *est2* cells harvested from 4th streak plate decreases more quickly than that seen with wildtype yeast cells. (B) Measurement of OD₆₀₀ of *est2* cells from four YPDA streak plates. Titters were 1 X 10⁷ cells/ml.

A similar experiment was performed on synthetic glucose complete media. Unlike rich media, it took approximately 45 minutes for 90% of the senescent cells to fall out of solution and during that time 70% of normal cells had also sedimented (Figure 35A). The rates of sedimentation of cells from each of the streaks displayed a different pattern compared to cells grown on rich YPDA media. The biggest changes occurred after the 3rd and 4th streaks on synthetic plates; in contrast, cells propagated on YPDA plates showed large changes after the 1st, 2nd and 3rd streaks and very little change between the 3rd and 4th streaks. This finding appears to be consistent with Neda Ghanem's studies indicating that cells grow faster in rich media than in synthetic media.

A



B

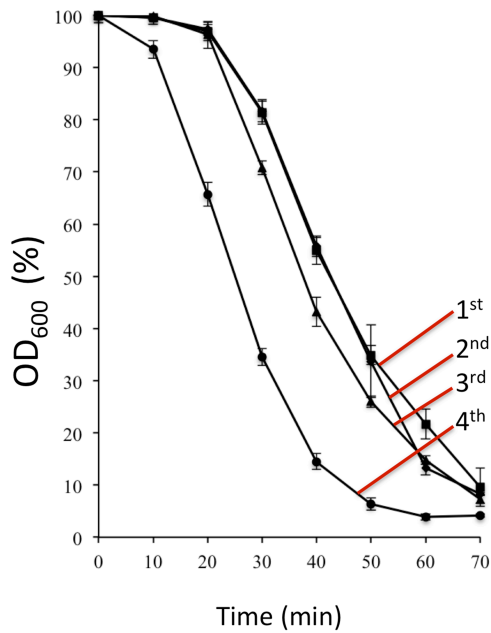


Figure 35. Older cells sediment more rapidly than normal cells after growth in synthetic media too. (A) Light scattering produced by *est2* cells harvested from 4th streak plates decreases more quickly than that seen with wildtype yeast cells. (B) Measurement of OD₆₀₀ of *est2* cells after each streak. Cell titers were 1 X 10⁷ cells/ml.

The next experiment measured the rate of sedimentation of *est2 rad52* cells that had been grown on rich media. In the case of *est2 rad52* cells, 80-90 % of cells from each streak fell out of solution at about 50 minutes, unlike *est2* cells, where cells from different streaks sedimented at different rates (Figure 36). Slight differences could be detected at the 50% level on the Y-axis, corresponding to the times needed to achieve a 50% reduction in the OD₆₀₀. The small changes may be because *est2 rad52* cells are bigger in size even in the early stages of senescence than *est2* cells. This result is consistent with the cell size experiment using *est2 rad52* cells (Figure 30), where average sizes of the 1st streak cells were approximately 8 μm , which is bigger than those of *est2* cells ($\sim 6 \mu\text{m}$).

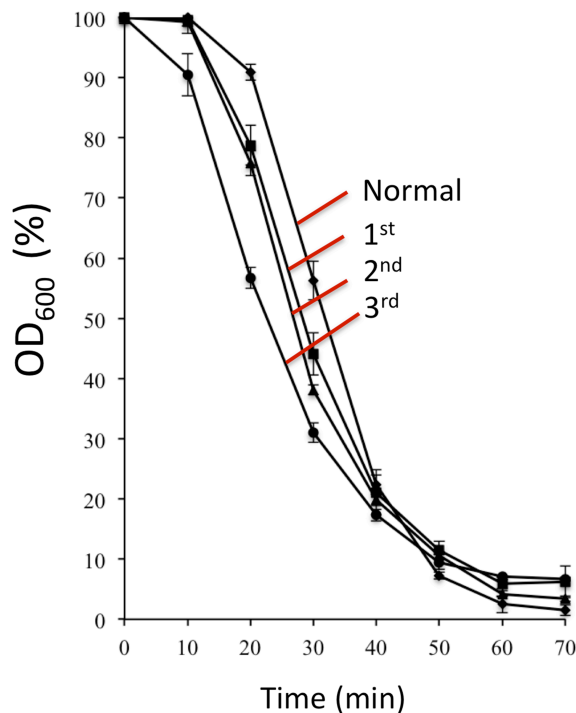
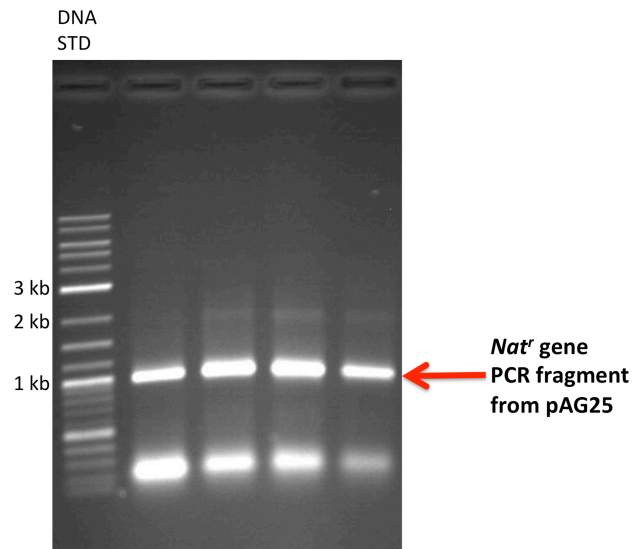


Figure 36. Measurement of changes in the OD₆₀₀ of *est2 rad52* cells at cell titer of 1×10^7 cells/ml after growth on rich media (YPDA).

An additional major goal of the current study was to use the special strain system to measure the effects of chemicals such as antioxidants and pro-oxidants on senescence rates. Creation of a hypersensitive strain that does not require high amounts of chemicals to be added to the growth media would improve these tests. This can be achieved by knocking out the pleiotropic drug resistance (PDR) genes *SNQ2* and *PDR5*, which encode membrane efflux transporters (33, 34). Cells lacking these transporters have reduced flow of chemicals out of the cells, therefore accumulating a higher concentration of drugs inside the cells. Past studies have shown increased drug sensitivity of cells by inactivation of the *PDR5* gene (33). Studies have also shown increased sensitivity of *pdr5 snq2* double mutants (34). In the past, undergraduate Lauren Morriss in our lab created strain YLKL1556 (YLKL803, *snq2Δ::G418^r*), which has a gene encoding resistance to the antibiotic *G418* inserted into the *SNQ2* gene.

In this study I created a double mutant strain by knocking out *PDR5* in strain YLKL1556. In this experiment, *E. coli* plasmid DNA for pAG25 was prepared using a QIAprep Spin Miniprep Kit. Then pAG25 containing the *Nat* (nourseothricin) resistance gene was PCR amplified using primers gPDR5A and gPDR5B. Both primers contain flanking sequences that are homologous to the sequence of the *PDR5* gene. The PCR product was confirmed through gel electrophoresis, where the size of the PCR fragment with the *Nat* gene was ~ 900 bp (Figure 37A). The PCR fragment was then transformed into yeast cells (YLKL1556), by using the rapid transformation of early stationary phase yeast cells protocol of Tripp *et al.* (37). The *Nat* gene was inserted in place of *PDR5* through homologous recombination (Figure 37B).

A



B

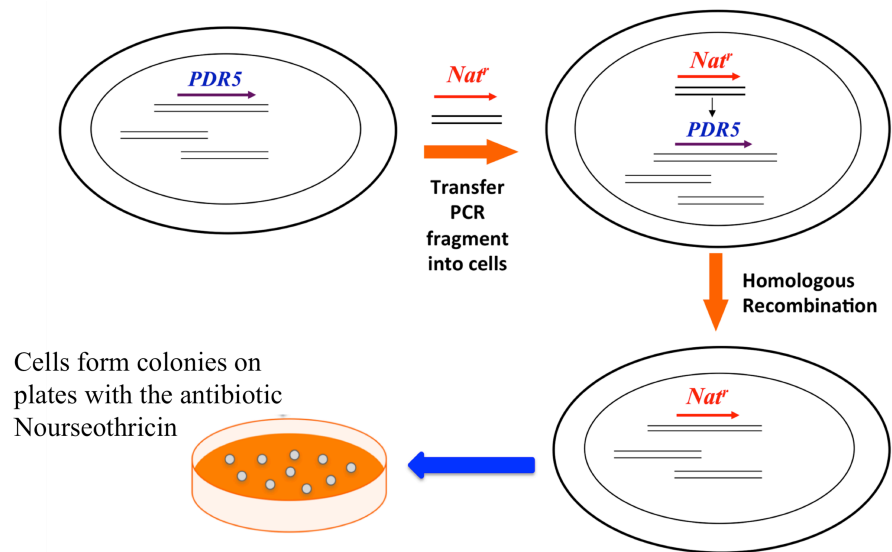


Figure 37. Creation of a hypersensitive strain. (A) Gel picture showing the PCR fragment containing the *Nat^r* gene. (B) Schematic diagram showing inactivation of *PDR5* by insertion of the *Nat^r* gene through homologous recombination.

Nat^r colonies formed after transformation were then used for chromosomal DNA purification. Proper insertion of the *Nat^r* gene was confirmed through PCR using 5pdr5 and 3pdr5 primers as test primers. Again, the PCR product was confirmed using gel electrophoresis. PCR fragments with the proper *Nat^r* gene insertion (*pdr5Δ::Nat^r*) were about ~ 1800 bp in size (Figure 38). The newly created strain, YLKL1558, now has both *SNQ2* and *PDR5* knocked out in the YLKL803 senescence strain background. This hypersensitive strain can be used to measure the effects of genetic and chemical factors on the rate of senescence more quantitatively.

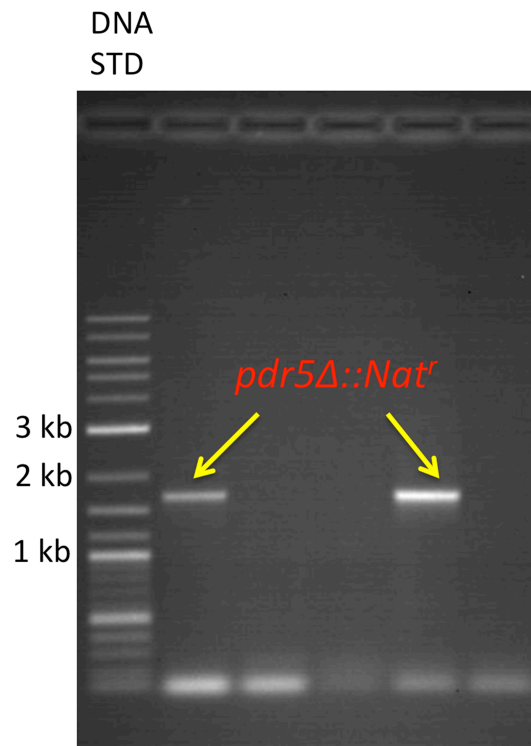


Figure 38. Gel picture showing proper insertion of the *Nat^r* gene into the *PDR5* locus in two isolates.

IV. SUMMARY AND CONCLUSIONS

The major goals of this project were to complete the development of a new quantitative assay for cell senescence and to measure changes in cellular morphology and cell division number during telomere-initiated senescence in the yeast *Saccharomyces cerevisiae*. Several studies have shown that telomere lengths in humans are affected by lifestyle choices; therefore humans of the same age can have different telomeric lengths (9, 10, 11). Past studies have also shown that older people with the shortest telomeres are at higher risk of developing age-related diseases (5). Studies have also shown an association between telomere shortening and oxidative damage. Oxidative stress and DNA damage caused by reactive oxygen species (ROS) in cells potentially increases the rate of telomere shortening (20-23). The yeast senescence assay system developed here should allow direct testing of chemical and genetic factors capable of influencing cell aging rates in eukaryotic cells, including the effects of ROS.

Following up on previous work in the current study (19, 29), the development and testing of a new statistics-based senescence plate assay was completed. The method involves counting the number of colonies on 3rd streak plates that can form full columns when streaked to a 4th streak plate. Senescence is a stochastic process, due to its random nature; there is considerable variability in the growth of cells on the 4th streak (Figure 6B). The new assay system addresses the problems caused by the variability. After performing several senescence assays with YLKL803 using the system, small improvements were made to reduce the randomness in the 4th streak. On the first 3 streaks plates, all second columns were streaked toward the outer edge of the plate so that

all cells would have proper access to nutrients and form larger colonies (Figure 8).

Another improvement made was to select more uniformly sized colonies (diameter ~ 0.8 mm) for streaking than in past experiments in a consistent manner (Figure 9).

In the current study, an alternative method to measure the rate of senescence was also investigated. The method uses a new strain that contains the pVL715 plasmid, which has *EST2* expression controlled by a constitutive promoter rather than a promoter regulated by galactose. Therefore, it is not necessary to switch cells from galactose to glucose. The results obtained using this strain (YLKL961) was similar to the results obtained using the original strain (YLKL803). In both of the strains senescence was observed on the 4th streak with a low number of full columns of growth. Approximately 2-3 full columns out of 8 columns on each plate were observed.

One of the major goals of the current project was to calculate the number of generations (cell divisions) undergone by the senescent cells before they stopped dividing. This work was a follow up of Neda Ghanem's experiments, where she used 9 inch Pasteur pipettes to harvest entire colonies from a plate surface. While following up on her work, I noticed that the diameter of the Pasteur pipette was sometimes equal to or smaller than the diameter of the colony being cored and sometimes not all of the cells were harvested from the colony. I also observed that a fraction of the cells were sticking to the walls of the Pasteur pipette and that pipetting up and down in water was necessary to get all of the cells out of the pipette. I determined that use of a long 1 ml plastic pipette in conjunction with an electronic pipettor could solve the problem caused by the small diameter of the Pasteur pipette. In subsequent experiments, 1 ml plastic pipettes were used to count the number of generations that cells went through during senescence on

both rich and synthetic media plates. These experiments revealed that telomerase-deficient cells (YLKL803) underwent 63-65 cell divisions before they senesced on the 4th streak plate. In contrast, homologous recombination-defective *rad52 est2* cells (YLKL807) underwent only ~ 40 cell divisions, exhibiting senescence on the 3rd streak plate.

The next major goal was to measure changes in cell morphology during aging, particularly changes in cell size. Past studies of yeast cell senescence have noted that, as cells age, they tend to become larger, while their telomere lengths get shorter (16, 18, 20). However, the magnitudes of these changes have never been quantitated before. The diameters of normal and senescent cells after each of the streaks (1st, 2nd, 3rd and 4th) were measured at both 400X and 1000X magnification. It was observed that cell size increased from ~ 6 μm after the 1st streak to ~ 10 μm in diameter during senescence. Telomerase-deficient YLKL803 cells typically showed a linear increase in size with time during senescence, though this was not always seen. Telomerase-deficient *rad52 est2* cells, on the other hand, were found to have bigger sizes at an earlier stage (1st streak) of approximately 8 μm , which is bigger than those of *est2* cells (~ 6 μm), and the *rad52* cells' sizes increased only modestly by the 4th streak.

Changes in the light scattering properties and the rate of sedimentation of cells during senescence were also assessed using spectrophotometry. Senescent cells exhibited greater light scattering than normal cells. The OD₆₀₀ of senescent cells was 21% and 32.6% higher than normal cells at 1 X 10⁶ cells/ml and 1 X 10⁷ cells/ml, respectively, likely because senescent cells are larger in size than normal cells (Figure 33). Older cells also sedimented much more rapidly than normal cells. Approximately 90% of senescent

cells fell out of solution within 30 minutes, while only 10% of normal cells were sedimented at that time. YLKL803 cells' rate of sedimentation after each plate streak was faster after growth on rich media than on synthetic media. The results showed a trend toward faster sedimentation after each streak. In the *rad52 est2* mutant cells, changes in the rate of sedimentation between each of the streaks were smaller. This result correlates with the cell size results and is likely due to the fact that *rad52* cells are bigger on the 1st streak than wildtype cells and exhibit only a modest increase in size by the end of senescence.

Another goal of my project was to create a hypersensitive strain system to measure the effects of chemicals on the rate of senescence. This was achieved by creating the double mutant strain YLKL1558 (YLKL803, *snq2Δ::G418^r pdr5Δ::Nat^r*). Creation of chemically hypersensitive strains should improve the usefulness of this senescence assay. Past studies have shown increased drug sensitivity of cells with an inactivation of the *PDR5* and *SNQ2* genes (33, 34). *SNQ2* and *PDR5* are pleiotropic drug resistance (PDR) genes, which encode membrane efflux ABC transporters (33, 34). Cells lacking these transporters reduce the flow of chemicals out of the cells, therefore accumulating higher concentrations of drugs inside. The newly created hypersensitive strain should allow measurement of the impacts of genetic and chemical factors on cell senescence more quantitatively than has ever been done before.

REFERENCES

1. Wellinger, R.J.; Zakian, V.A. *Genetics* **2012**, 191, 1073-1105.
2. Moyzis, R. K.; Buckingham, J.M.; Cram, L.S.; Dani, M.; Deaven, L.L.; Jones, M.D.; Meyne, J.; Ratliff, R.L.; Wu, J. *Biochemistry* **1988**, 85, 6622-6626.
3. Greider, C.W.; Blackburn, E.H. *Nature* **1989**, 337, 331-337.
4. Greider, C.W.; Blackburn, E. H. *Cell* **1985**, 43, 405-413.
5. Cawthon, R. M.; Smith, K. R.; O'Brien, E.; Sivatchenko, A.; Kerber, R. A. *Lancet* **2003**, 361, 393-395.
6. Campisi, J.; Fagagna, F. *Nature Reviews Molecular Cell Biology* **2007**, 8, 729-740.
7. Hardin, J.; Bertoni, G. P.; Kleinsmith, L.J., Becker's World of the Cell, **2012**.
8. Yaffe, K.; Lindquist, K.; Kluse, M.; Cawthon, R.; Harris, T.; Hsueh, W.; Simonsick, E.M.; Kuller, L., Li, R.; Ayonayon, H.N.; Rubin, S. M.; Cummings, S.R. *Neurobiology of Aging* **2009**, 32, 2055-2060.
9. Huzen *et al.* *Journal of Internal Medicine* **2014**, 275, 155-163.
10. LaRocca, T.J.; Seals, D.R.; Pierce, G.L. *Mechanism of Aging and Development* **2010**, 131, 165-167.
11. Paul, L. *Journal of Nutritional Biochemistry* **2011**, 22, 895-901.
12. Kim, N.M.; Pietyszek, M.A.; Prowse, K.R.; Harley, C.B.; West, M.D.; Ho, P.L.; Coviello, G.M.; Wright, W.E.; Weinrich, S.L.; Shay, J.W. *Science* **1994**, 266, 2011-1015.
13. Ruden, M.; Puri, N. *Cancer Treatment Reviews* **2013**, 39, 444-456.
14. Lundblad, V, Budding yeast telomeres, in: Telomeres, Cold Spring Harbor Laboratory Press, **2006**, 345-386.
15. Smogorzewska, A; Lange, T. *Biochemistry* **2004**, 73, 177-208.
16. Becerra, S. C.; Thambugala, H. T.; Erickson, A. R.; Lee, C. K.; Lewis, L.K. *DNA Repair* **2012**, 11, 35-45.
17. Lundblad, V.; Blackburn, E. H. *Cell* **1993**, 73, 347-360.

18. Enomoto, S.; Glowczewski, L.; Berman, J. *Molecular Biology of the Cell* **2002**, 13, 2626-2638.
19. Ghanem, N. Z. Telomere-initiated cellular aging in *Saccharomyces cerevisiae*: impact of nutrient availability and factors affecting genetic exchange, Master's Thesis, Texas State University, **2015**.
20. Ijpma, A.S.; Greider, C. W. *Molecular Biology of the Cell* **2003**, 14, 987-1001.
21. Furumoto, K.; Inoue, E.; Nagao, N.; Hiyama, E.; Miwa, N. *Life Sciences* **1998**, 63, 935-948.
22. Melov, S.; Ravenscroft, J.; Malik, S.; Gill, M. S.; Walker, D. W.; Clayton, P. E.; Wallace, D.C.; Malfroy, B.; Doctrow, S. R.; Lithgow, G.J. *Science* **2000**, 289, 1567-1569.
23. Chen, J.; Hales, C. N.; Ozanne, S.E. *Nucleic Acids Research* **2007**, 35, 7417-7428.
24. Sonoda, E.; Hohegger, H.; Saberi, A.; Taniguchi, Y.; Takeda, S. *DNA Repair* **2006**, 5 1021-1029.
25. Wyman, C.; Kanaar, R. *Annu. Rev. Genet* **2006**, 40, 363-83.
26. Filippo, J. S.; Dung, P.; Klin, H. *Annu. Rev. Biochem.* **2008**, 77, 229-57.
27. Game, J.C. *Mutation Research* **2000**, 451, 277-293.
28. Ballew, B. J.; Lundblad, V. *Aging Cell* **2013**, 12, 719-727.
29. Araki, N. Improved methods for analysis of telomere of telomere-initiated cellular senescence and telomere shortening in *Saccharomyces cerevisiae*, Master's Thesis, Texas State University, **2011**.
30. Lodish, H. *et al.* *Molecular Cell Biology*, 4th ed.; W.H. Freeman and Company: New York, **2000**, 146-147.
31. Vera, E.; Bernardes de Jesus, B.; Foronda, M.; Flores, J.M.; Blasco, M.A. *PLoS One* **2013**, 8.
32. Teixeira, M. T. *Frontiers in Oncology* **2013**, 3,101.
33. Zhang, M.; Liang, Y.; Zhang, X.; Xu, Y.; Dai, H.; Xiao, W. *Toxicological Sciences* **2008**, 103, 68-76.

34. Zhang, M.; Hanna, M.; Li, J.; Butcher, S.; Dai, H.; Xiao, W. *Toxicological Sciences* **2010**, 113, 401-411.
35. Brachmann, C.B.; Davies, A.; Cost, G.J.; Caputo, E.; Li, J.; Hieter, P.; Boeke, J.D. *Yeast* **1998**, 14, 115-132.
36. Goldstein, A.L.; McCusker, J.H. *Yeast* **1999**, 15, 1541-1553.
37. Tripp, J. D.; Lilley, J. L.; Wood, W. N.; Lewis, L.K. *Yeast* **2013**, 30, 191-200.
38. Lee, C.K.; Araki, N.; Sowersby, D.S.; Lewis, L.K. *Yeast* **2012**, 29, 73-80.
39. Nugent, C. I.; Bosco, G.; Ross, L. O.; Evans, S. K.; Salinger, A. P.; Moore, J. K.; Haber, J. E.; Lundblad, V. *Current Biology* **1998**, 8, 657-662.